NOAA Technical Report NESDIS 36

# Pre-Launch Calibration of Channels 1 and 2 of the Advanced Very High Resolution Radiometer

Washington, D.C.
October 1987

**U.S. DEPARTMENT OF COMMERCE**
**National Oceanic and Atmospheric Administration**
National Environmental Satellite, Data, and Information Service

NOAA Technical Report NESDIS 36

# Pre-Launch Calibration of Channels 1 and 2 of the Advanced Very High Resolution Radiometer

C.R. Nagaraja Rao
Satellite Research Laboratory
National Environmental Satellite, Data, and Information Service
Washington, D.C. 20233

October 1987



**U.S. DEPARTMENT OF COMMERCE**
**C. William Verity, Secretary**

**National Oceanic and Atmospheric Administration**
J. Curtis Mack II, Acting Under Secretary

National Environmental Satellite, Data, and Information Service
Thomas N. Pyke, Assistant Administrator

TABLE OF CONTENTS

List of Figures

## List of Tables

# PRE-LAUNCH CALIBRATION OF CHANNELS 1 AND 2 OF THE ADVANCED VERY HIGH RESOLUTION RADIOMETER

C.R.Nagaraja Rao

National Oceanographic and Atmospheric Administration

National Environmental Satellite, Data, and Information Service

Washington, D.C. 20233

## Abstract

The basic physical principles underlying the pre-launch calibration of Channels 1 and 2 of the Advanced Very High Resolution Radiometer(AVHRR) are presented and discussed. The laboratory procedures for the calibration of the NASA 30-inch intergrating sphere source and for the establishment of a simple linear regression relationship between the reflectance factor of the integrating sphere source and the AVHRR digital signals in Channels 1 and 2 corresponding to different levels of illumination (of the integrating sphere source) are described in detail. The effects on this regression relationship of using extraterrestrial solar spectral irradiance data different from the Thekaekara(1974) data that have been used in the determination of the reflectance factor of the integrating sphere source are briefly mentioned. The method of using the above-mentioned regression relationship to determine the reflectance factor of the earth-atmosphere scene viewed by the AVHRR is outlined.

## 1. Introduction

In the course of the development and application of aerosol remote sensing using the radiances measured in Channels 1 and 2 of the Advanced Very High Resolution Radiometer(AVHRR) onboard the NOAA polar orbiting environmental satellites, the need for information on the pre-launch calibration of these two channels was keenly felt. Details of the various calibration procedures and of the underlying physical principles were not widely known nor were they easily accessible. We have therefore undertaken the task of compiling in this report relevant information obtained from diverse sources such as NOAA technical reports and memoranda, contractor reports, operating procedures developed under contract with NASA and NOAA and correspondence between scientists at NOAA, NASA and at ITT Aerospace/Optical Division, Fort Wayne, Indiana.

We shall first give a brief description of the Advanced Very High Resolution Radiometer. This will be followed by a presentation of the underlying theory for establishing a simple linear regression relationship between the reflectance factor of the earth-atmosphere scene being viewed by the AVHRR and the AVHRR digital signals in terms of the reflectance factor of an integrating sphere source. We shall then discuss in detail the calibration of the NASA 30-inch integrating sphere source and of Channels 1 and 2 of the AVHRR in the laboratory. We shall conclude with a discussion of the effects on the above-mentioned regression relationship of using extraterrestrial solar spectral irradiance data different from the Thekaekara(1974) data that have

been used in the calibration of the integrating sphere source.

2. The Advanced Very High Resolution Radiometer(AVHRR)

The Advanced Very High Resolution Radiometer is a broad-band filter radiometer designed to make measurements of the upwelling radiance from the earth-atmosphere system in the visible, near- and thermal infrared regions of the spectrum. Measurements can be made in either 4(Model 1) or 5(Model 2) spectral intervals.The modular structure of the AVHRR facilitates design changes to be incorporated without perceptibly altering the physical configuration of the instrument and its interface with the satellite. The five modular units that constitute the AVHRR are: the optical subsystem, the scan system, electronics subsystem, radiant cooler module, and the baseplate; these are shown in Fig.1.

The optical sub-system, which is of primary interest to us, is built around an 8-inch aperture, afocal, Cassegrain telescope made up of two coaxial paraboloidal mirrors. The collimated beam emerging from the telescope passes through an optical train(Fig.2) consisting of beam splitters, folding mirrors, and reimaging lenses which separate and channel the incoming beam into the various spectral intervals defined by broad-band interference filters which are assumed to have wavelength-independent transmission characteristics over the spectral intervals of interest. The spectrally isolated beam then impinges upon an appropriate detector. Square silicon detectors, 0.10" on the side, are employed in Channels 1(visible) and 2(near-infrared);

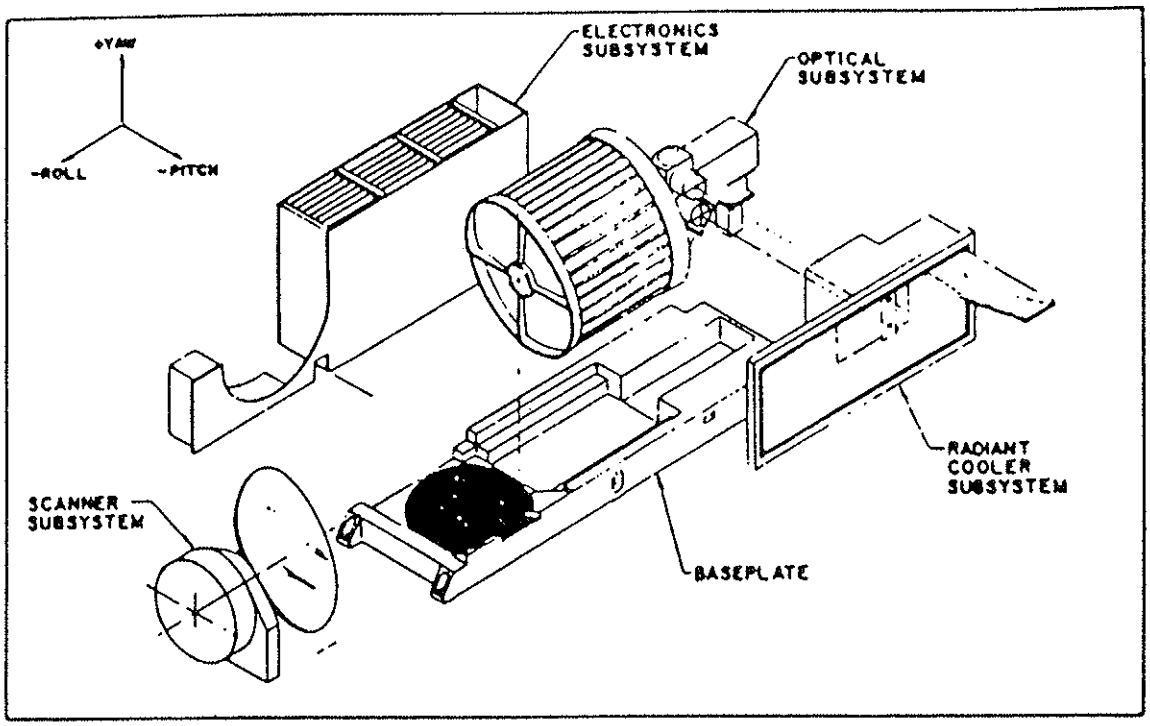


Figure 1. Exploded view of the subsystems of the Advanced Very High Resolution Radiometer

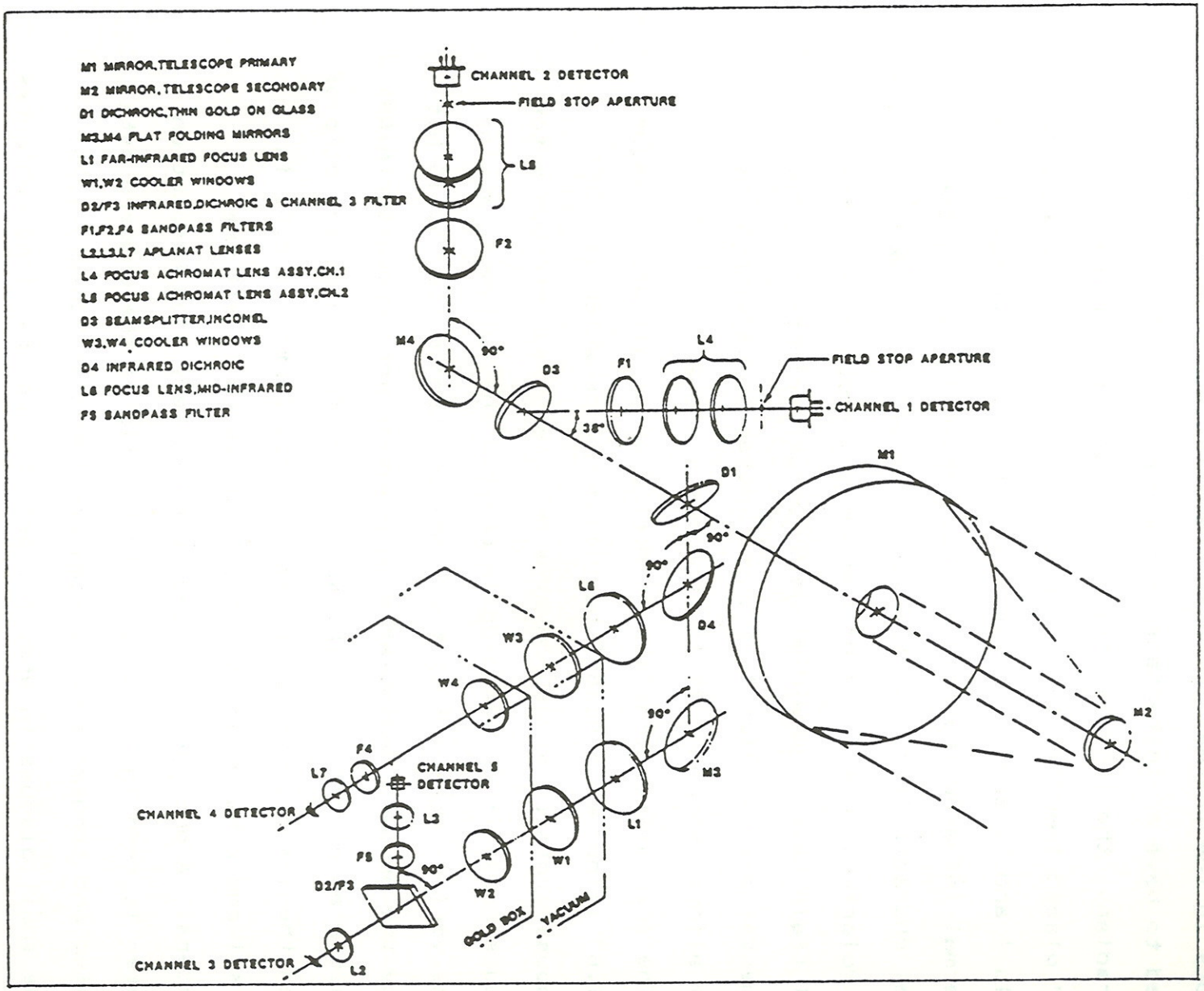


Figure 2. Optical subsystem of the 5-Channel version of the AVHRR

and cooled mercury-cadmium-telluride and indium-antimonide detectors in the thermal infrared channels. All channels are designed to have an instantaneous field of view(IFOV) of 1.3 milli-radians; the IFOV is defined by a square aperture of side 0.0238" placed immediately in front of the silicon detectors in Channels 1 and 2; and by the active area of the detector itself in the thermal infrared channels. We have shown in Table 1 the spectral characteristics of the passbands of the two models of the AVHRR. Polarization effects of the various components of the optical train have been minimized by proper orientation; the instrumental polarization is thus estimated to be within the maximum allowed value of 7% in Channels 1 and 2.

The scan system consists primarily of an elliptical(major axis:11.6" ;minor axis:8.36") beryllium mirror which is continuously rotated at 360rpm by a hysteresis synchronous motor to produce cross-track scanning in orbit. The voltages issuing from the various channels of the AVHRR are transmitted as 10-bit words by the onboard Manipulated Information Rate Processor(MIRP) and associated electronics. The specified signal to noise ratio of 3:1 when the integrating sphere reflectance factor is 0.5% in Channels 1 and 2 has been attained or exceeded in all the radiometers. A photograph of the Advanced Very High Resolution Radiometer is seen in Fig.3. Greater details of the onboard data processing and transmission systems are found in Schwalb(1978).

We shall discuss in what follows how the upwelling radiances from the earth-atmosphere system in the passbands of AVHRR

Table 1. Spectral bandpass characteristics of the AVHRR

| Model | Channel 1 | 2 | 3 | 4 | 5 |
|---|---|---|---|---|---|
| 1 | 0.57-0.69 μm | 0.72-0.98 μm | 3.55-3.95 μm | 10.4-11.4 μm | - |
| 2 | 0.57-0.69 μm | 0.72-0.98 μm | 3.55-3.95 μm | 10.4-11.4 μm | 11.4-12.4 μm |

Notes: 1. The wavelengths, in units of micrometer, correspond nominally to the 50% normalized spectral response points.
2. See Figs.7-11 for detailed spectral response curves of the AVHRRs on NOAA 6-10 spacecraft.

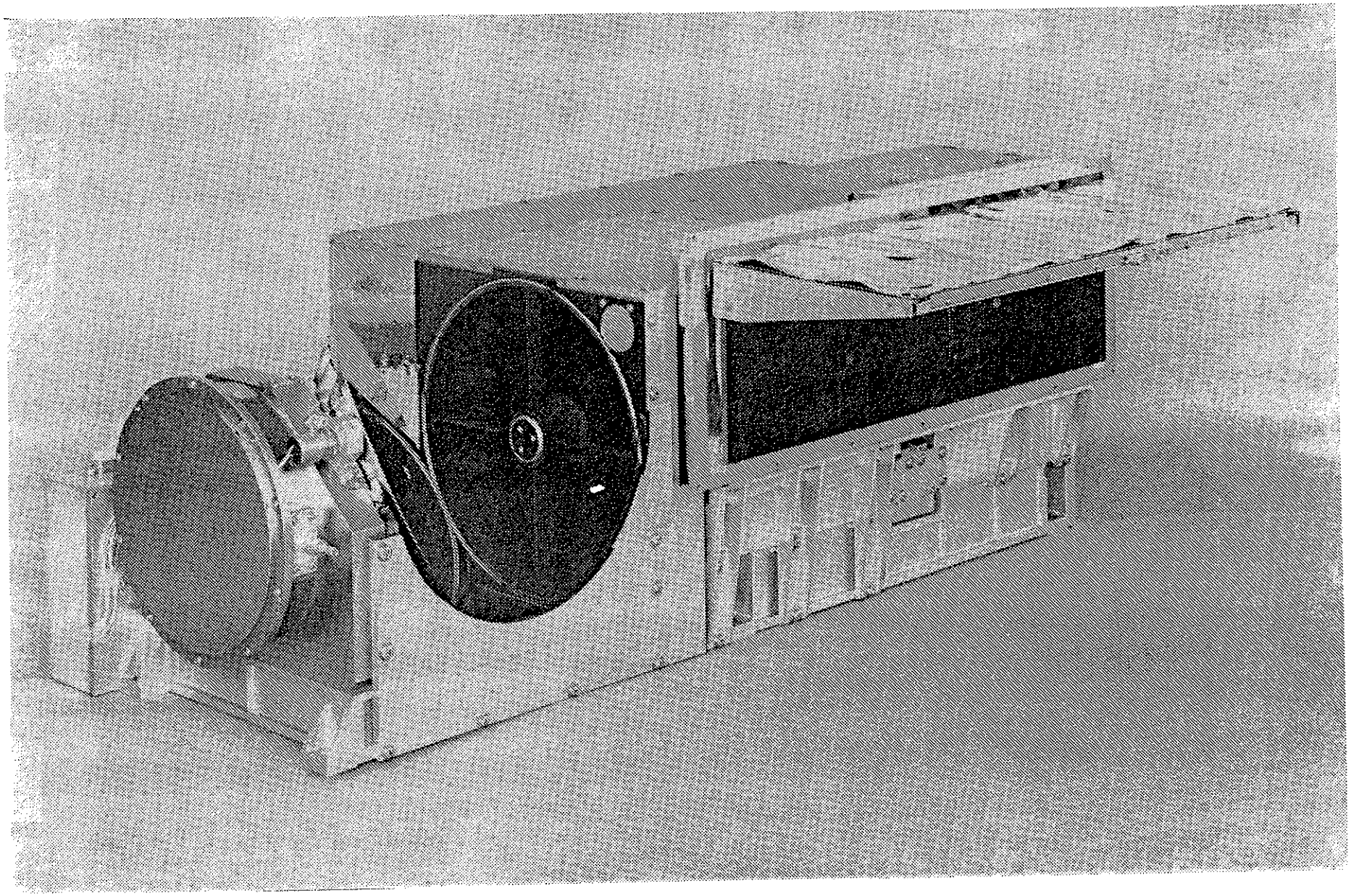

Figure 3. The Advanced Very High Resolution Radiometer

Channels 1 and 2 can be estimated using the simple linear regression relationship established in the laboratory between the variable radiances of an integrating sphere source and the corresponding AVHRR digital signals.

## 3. Basic theory of the pre-launch calibration of AVHRR Channels 1 and 2

It has been the usual practice to express the radiances measured in AVHRR Channels 1 and 2 in terms of an 'albedo' which relates the measured radiance to the filtered extraterrestrial solar irradiance in the passband of a given channel. In the light of accepted meteorological usage, we feel the term 'albedo' should be used exclusively to denote the ratio of the upward and downward fluxes of radiation at a surface; we shall therefore use the term 'reflectance factor' in its stead in this report.

Let the filtered radiance $I(Wm^{-2}sr^{-1})$ when the AVHRR is viewing the integrating sphere source be given by

$$I = \int_{\lambda_1}^{\lambda_2} S_\lambda \tau_\lambda d\lambda \qquad (1)$$

where $S_\lambda$ : the radiance of the integrating sphere source at the wavelength $\lambda$ ;

$\tau_\lambda$ : the normalized response function of the given channel at the wavelength $\lambda$ ;

and $\lambda_1, \lambda_2$ : the cut-on and cut-off wavelengths of the passband of

the given channel. We shall define the filtered extraterrestrial solar irradiance($Wm^{-2}$) as

$$F = \int_{\lambda_1}^{\lambda_2} F_{o\lambda} \tau_\lambda d\lambda \qquad (2)$$

where $F_{o\lambda}$ is the extraterrestrial solar spectral irradiance at the wavelength $\lambda$.

Other quantities of interest are the mean or effective wavelength

$$\overline{\lambda} = \int_{\lambda_1}^{\lambda_2} \lambda F_{o\lambda} \tau_\lambda d\lambda \Big/ F \qquad (3)$$

and the equivalent channel width

$$w = \int_{\lambda_1}^{\lambda_2} \tau_\lambda d\lambda \qquad (4)$$

The reflectance factor $A$ of the integrating sphere source is defined as the ratio

$$A = \frac{\pi I}{F} \qquad (5)$$

The reflectance factor can thus be interpreted as the ratio of the irradiance of an isotropic radiation field with radiance $I$ (the measured filtered radiance) to the filtered solar irradiance.

As mentioned earlier, the basic objective of the pre-launch calibration has been to establish a simple linear regression relationship between the reflectance factor A, expressed as a percentage, of the integrating sphere source corresponding to different levels of illumination and the AVHRR digital signal C, in counts; thus,

$$A(\%) = a(\%) + b(\%/\text{count})C(\text{counts}) \quad (6)$$

A similar regression relationship for the filtered integrating sphere radiance $I(Wm^{-2}sr^{-1})$ will be

$$I = a' + b'C \quad (7)$$

where $a' = Fa / 100\,\pi \quad (Wm^{-2}sr^{-1})$

and $b' = Fb / 100\,\pi \quad (Wm^{-2}sr^{-1}count^{-1})$

The spectral radiance $I'(Wm^{-2}\mu m^{-1}sr^{-1}) = I/w$ is then related to the AVHRR digital signal by

$$I' = a'' + b''C \quad (8)$$

where

$$a'' = Fa/100\,\pi w \quad (Wm^{-2}\mu m^{-1}sr^{-1})$$

and $$b'' = Fb/100\,\pi w \quad (Wm^{-2}\mu m^{-1}sr^{-1}count^{-1}).$$

In a manner analogous to Eqn.5, we can define the reflectance factor $A_e$ of the earth-atmosphere scene being viewed by the AVHRR in orbit as

$$A_e = \pi \int_{\lambda_1}^{\lambda_2} I_\lambda \tau_\lambda d\lambda \Big/ F = \frac{\pi I_e}{F} \qquad (9)$$

where $I_\lambda$ : radiance of the earth-atmosphere scene at the wavelength $\lambda$.

It has been the practice to estimate $A_e$, expressed as a percentage, and subsequently, the corresponding radiance $I_e$, using the transmitted AVHRR signals in the relationship given in Eqn.6. It is thus tacitly assumed that the radiometer response is sensitive only to the total amount of radiant energy that is sensed by the instrument within the passband of the channel and not to the spectral energy distribution of the scene radiance over the passband.

The filtered radiance $I_e (Wm^{-2}sr^{-1})$ of the earth-atmosphere scene is given by

$$I_e = (FA_e)/100\,\pi \qquad (10)$$

and the corresponding spectral radiance $I_e' (Wm^{-2}\mu m^{-1}sr^{-1})$ by

$$I_e' = I_e/w \qquad (11)$$

It is important that the F values used in Eqns. 10 and 11 are based on the spectral solar irradiance data that were used in Eqn.2.

We see from the above that the laboratory calibration of channels 1 and 2 of the AVHRR is essentially directed towards the estimation of the radiance of the earth-atmosphere scene in terms

of the radiance of the integrating sphere source. We shall now describe the various stages and procedures of establishing the afore-mentioned regression relationship.

## 4. The NASA 30-inch Integrating Sphere Source

### 4.1 General

The NASA 30-inch Integrating Sphere Source, hereafter referred to simply as the integrating sphere, has been extensively used by ITT Aerospace/Optical Division, the AVHRR manufacturer, in the pre-launch calibration of Channels 1 and 2 of the AVHRR. The inside of the sphere is coated with barium sulphate with a diffuse reflectivity very close to unity and can be illuminated with up to 12 quartz-halogen lamps matched, to the extent practicable, for spectral output and operating current. The radiance at the 12-inch exit aperture of the integrating sphere approximates very closely that of an isotropic radiation field; it can be varied by changing the number of lamps used to illuminate the inside of the sphere.

### 4.2 Spectral radiance of the integrating sphere

Available records indicate that the integrating sphere was calibrated in the laboratory for linearity of output and spectral radiance initially in 1974, and again in 1983(R.Koczar, personal communication). The operational regression relationships between the scene reflectance factor and AVHRR counts( vide Sec.3) for NOAA-6 through NOAA-10 are based on the calibration of the integrating sphere performed in 1974. However, because of the unavailability of some of the relevant documentation for the 1974 calibration, we shall outline the method of determination of

spectral radiance and linearity of output of the integrating sphere using in the main data obtained during the calibration performed in 1983. An Optronic Laboratories Model 740A Optical Radiation Measurement System, essentially consisting of a single-grating monochromator with interchangeable gratings to cover the spectral region from 0.35 to 2.0um, and equipped with interchangeable uv-enhanced silicon and thermoelectrically cooled germanium detectors, and an IR blocking filter, was used to compare the spectral output of the integrating sphere to that of an Optronic Laboratories Model 420 continuously variable integrating sphere source which in turn had been calibrated for spectral radiance over the 0.35-2um wavelength region relative to the National Bureau of Standards(NBS) radiance and spectral irradiance scale. The estimated uncertainty in the calibration of the Model 420 calibration source relative to the NBS standards is given in Table 2.

Table 2. Uncertainty in the Model 420 calibration source

| Spectral Interval | Uncertainty(%) |
|---|---|
| 0.35-0.40um | 3 |
| 0.40-0.90um | 2 |
| 0.90-1.30um | 3 |
| 1.30-2.00um | 4 |

The radiometric quantities measured as part of the calibration of the integrating sphere are the near-normal spectral radiance of the 12-inch aperture and the relative radiances at selected wavelengths as the number of lamps illuminating the sphere is changed from 12 to 1 in steps of 1. The spectral radiance measurements have been made at 0.05μm intervals over the spectral region of interest. It has been estimated that the uncertainty in the transfer calibration from the Optronic Laboratories Model 420 continuously variable integrating sphere source to the NASA integrating sphere is 1.5%.

We have shown in Table 3 the measured values of the near-normal spectral radiance of the integrating sphere when it was illuminated with 12 lamps. Assuming that the integrating sphere is an isotropic source of radiation, the spectral irradiances are calculated as $\pi$ times the spectral radiances. The discrepancies between the radiances measured at wavelengths common to the calibrations performed in 1974 and 1983 may in part be due to the fact that the integrating sphere was dis-assembled and repainted prior to the 1983 calibration(R.Koczar, personal communication) and to the differences in the calibration procedures adopted.

The relative variations in the integrating sphere radiances at the wavelengths of 0.45 and 0.55μm as the number of lamps was changed from 12 to 1 in steps of 1 have also been studied. It is observed that the mean and standard deviation of the ratio

Table 3. Near-normal spectral radiance of the NASA 30-inch integrating sphere source

| Wavelength ($\mu m$) | Spectral Radiance ($Wm^{-2}\mu m^{-1}sr^{-1}$) | |
|---|---|---|
| | a | b |
| 0.500 | 178.2 | 180.0 |
| 0.550 | - | 264.0 |
| 0.600 | 349.7 | 351.0 |
| 0.650 | - | 429.0 |
| 0.700 | 487.8 | 505.0 |
| 0.750 | - | 568.0 |
| 0.800 | 618.8 | 606.0 |
| 0.850 | - | 610.0 |
| 0.900 | 655.5 | 613.0 |
| 0.950 | - | 606.0 |
| 1.000 | - | 602.0 |
| 1.050 | 569.8 | 589.0 |
| 1.100 | - | 560.0 |

Notes:
1. Values in column "a" are based on the 1974 calibration of the integrating sphere.
2. Values in column "b" are based on the 1983 calibration of the integrating sphere.
3. The spectral irradiance($Wm^{-2}\mu m^{-I}$) is given by $\pi$ times the spectral radiance.

$(I_n/I_{12})/(n/12)$, where $I_n$ and $I_{12}$ are the integrating sphere radiances when illuminated with $n(n \leq 12)$ and 12 lamps respectively, have values of 1.0026 and 0.0042 at 0.45μm; and 1.0011 and 0.0047 at 0.55μm; these numbers can be considered a measure of the linearity of the integrating sphere source in the visible region of the spectrum.

We have compared in Table 4 the spectral irradiances of the integrating sphere and of the sun. The Air Force(1965) solar spectral irradiance data are based on irradiances tabulated over spectral intervals ranging from 0.01 to 0.02μm centred on the wavelength of interest; the Thekaekara(1974) data are based on irradiance tabulations at 0.005μm intervals upto 0.6μm; at 0.01μm intervals between 0.6 and 1.0μm; and at 0.05μm intervals at longer wavelengths; the Neckel and Labs(1984) data, taken from Rossow et al.(1985), are based on irradiances averaged over 0.01μm intervals centered on the wavelength of interest; these data will be utilized to demonstrate the dependence of the reflectance factor of the integrating sphere on the solar spectral irradiances used.

We have shown in Fig.4 the spectral variation of the integrating sphere and solar irradiances from 0.50 to 1.07μm. It is apparent that the sphere and solar irradiances vary with wavelength in opposite senses, with the cross-over point lying around 0.69μm. This wavelength dependence of the integrating sphere irradiance is such that the filtered sphere irradiance in Channel 2 when the sphere is illuminated with 12 lamps is very

Table 4. Spectral irradiances($Wm^{-2}\mu m^{-1}$) of the sun and integrating sphere

| WAVELENGTH | AIRFORCE | THEKAEKARA | NECKEL & LABS | INT. SPHERE |
|---|---|---|---|---|
| .5 | 2005 | 1942 | 1921 | 565.5 |
| .51 | 1945 | 1882 | 1929 | 618.3 |
| .52 | 1925 | 1833 | 1824 | 671.1 |
| .53 | 1960 | 1842 | 1876 | 723.9 |
| .54 | 1980 | 1783 | 1876 | 776.6 |
| .55 | 1949 | 1725 | 1878 | 829.4 |
| .56 | 1910 | 1695 | 1844 | 884.1 |
| .57 | 1907 | 1712 | 1846 | 938.7 |
| .58 | 1909 | 1715 | 1848 | 993.4 |
| .59 | 1900 | 1700 | 1785 | 1048 |
| .6 | 1818.6 | 1666 | 1772 | 1102.7 |
| .61 | 1774.5 | 1635 | 1736 | 1151.7 |
| .62 | 1737.5 | 1602 | 1696 | 1200.7 |
| .63 | 1701 | 1570 | 1668 | 1249.7 |
| .64 | 1663.5 | 1544 | 1637 | 1298.7 |
| .65 | 1625.5 | 1511 | 1584 | 1347.7 |
| .66 | 1588.5 | 1486 | 1528 | 1395.5 |
| .67 | 1552 | 1456 | 1530 | 1443.2 |
| .68 | 1515.5 | 1427 | 1490 | 1491 |
| .69 | 1479.5 | 1402 | 1456 | 1538.7 |
| .7 | 1444.5 | 1369 | 1410 | 1586.5 |
| .71 | 1411 | 1344 | 1386 | 1626.1 |
| .72 | 1376 | 1314 | 1345 | 1665.7 |
| .73 | 1340 | 1290 | 1327 | 1705.2 |
| .74 | 1306.5 | 1260 | 1285 | 1744.8 |
| .75 | 1273.5 | 1235 | 1269 | 1784.4 |
| .76 | 1241.5 | 1211 | 1240 | 1808.3 |
| .77 | 1213 | 1185 | 1201 | 1832.2 |
| .78 | 1183.5 | 1159 | 1188 | 1856 |
| .79 | 1153.5 | 1134 | 1160 | 1879.9 |
| .8 | 1126.5 | 1109 | 1138 | 1903.8 |
| .81 | 1100.5 | 1085 | 1113 | 1906.3 |
| .82 | 1075.5 | 1060 | 1082 | 1908.8 |
| .83 | 1051.5 | 1036 | 1063 | 1911.4 |
| .84 | 1027.5 | 1013 | 1041 | 1913.9 |
| .85 | 1003.5 | 990 | 971 | 1916.4 |
| .86 | 980.5 | 968 | 996 | 1918.3 |
| .87 | 958 | 947 | 950 | 1920.2 |
| .88 | 936.5 | 926 | 984 | 1922 |
| .89 | 916 | 908 | 964 | 1923.9 |
| .9 | 895.5 | 891 | 943 | 1925.8 |
| .91 | 875.5 | 880 | 923 | 1921.4 |
| .92 | 856.5 | 869 | 904 | 1917 |
| .93 | 838 | 858 | 884 | 1912.6 |
| .94 | 820.5 | 847 | 866 | 1908.2 |
| .95 | 803.5 | 837 | 848 | 1903.8 |
| .96 | 786.5 | 820 | 830 | 1901.3 |
| .97 | 770 | 803 | 812 | 1898.8 |
| .98 | 754.5 | 785 | 794 | 1896.2 |
| .99 | 739.5 | 767 | 777 | 1893.7 |
| 1 | 725.5 | 748 | 760 | 1891.2 |
| 1.01 | 712.5 | 732 | 743 | 1883 |
| 1.02 | 700 | 716 | 726 | 1874.9 |
| 1.03 | 688 | 700 | 710 | 1866.7 |
| 1.04 | 676 | 684 | 693 | 1858.6 |
| 1.05 | 664 | 668 | 676 | 1850.4 |
| 1.06 | 652 | 653 | 664 | 1832.2 |
| 1.07 | 640.5 | 638 | 654 | 1814 |

Note: Wavelengths are in units of micrometer.

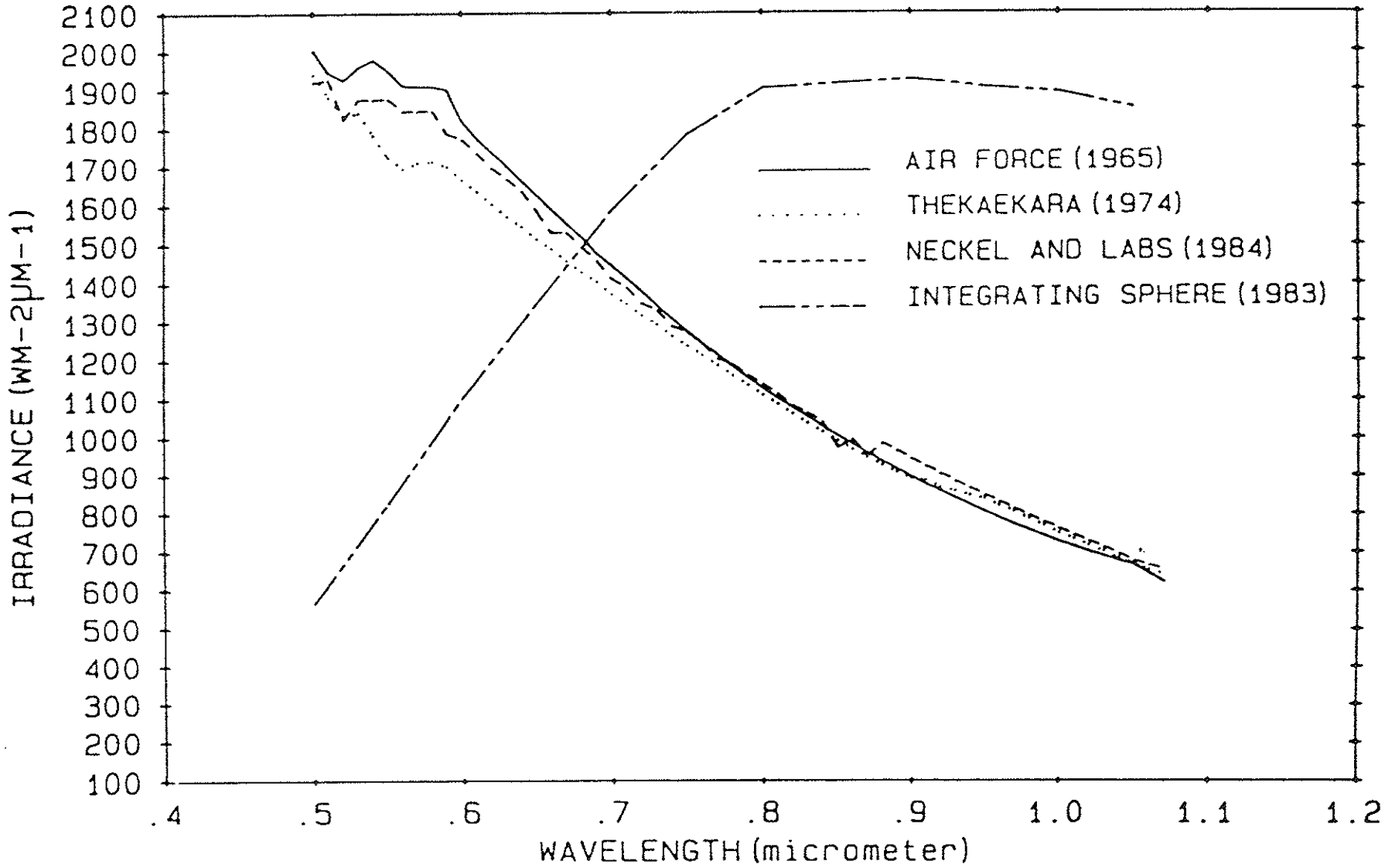


Figure 4. Spectral irradiances of the sun and the integrating sphere

nearly double the filtered solar irradiance in this channel; thus, in practice, since the reflectance factor $A \leq 1$, all calibrations of Channel 2 are performed with the sphere illuminated with upto 6 lamps only.

4.3 The sphere ratio

The "sphere ratio", assumed to be independent of wavelength, is used to calculate the reflectance factor of the integrating sphere at different levels of illumination, given the reflectance factor at the highest level of illumination(12 lamps for Channel 1; 6 lamps for Channel 2). It is defined as the normalized relative radiance of the integrating sphere at the wavelength of 0.55μm (at the corresponding levels of illumination), the normalization factor being the relative radiance at 0.55μm at the highest level of illumination. We have shown in Table 5 the measured sphere ratios based on the 1974 and 1983 calibrations of the integrating sphere; we have also included in the table the ratios n/12 and n/6, n being the number of lamps; these are referred to as the calculated sphere ratios.

It is apparent there is very close correspondence, except at low levels of illumination($n \leq 2$ for Channel 1; $n=1$ for Channel 2), between the two sets of measured sphere ratios, and between the measured and calculated values. Regression of the measured on the calculated sphere ratios yields slopes very close to unity and coefficients of determination in excess of 0.99; similar values for the regression parameters are obtained when the 1983 sphere ratios are regressed on the 1974 values. It is thus reasonable to

assume that the integrating sphere is a linear source of illumination; however, we cannot comment upon the stability of spectral radiance of the integrating sphere as a function of time because of the sparsity of data and of the fact the sphere was dis-assembled and repainted between the two calibrations performed in 1974 and 1983.

Table 5. Measured and calculated sphere ratios

| Number of lamps(n) | Sphere ratio: Observed: Channel 1 a | Channel 1 b | Channel 2 a | Channel 2 b | Calculated: Channel 1 (n/12) | Channel 2 (n/6) |
|---|---|---|---|---|---|---|
| 12 | 1.0000 | 1.0000 | | - | 1.0000 | - |
| 11 | 0.9154 | 0.9160 | | - | 0.9167 | - |
| 10 | 0.8334 | 0.8340 | | - | 0.8333 | - |
| 9 | 0.7504 | 0.7510 | | - | 0.7500 | - |
| 8 | 0.6647 | 0.6690 | | - | 0.6667 | - |
| 7 | 0.5801 | 0.5850 | | - | 0.5833 | - |
| 6 | 0.4949 | 0.5040 | 1.0000 | 1.0000 | 0.5000 | 1.0000 |
| 5 | 0.4130 | 0.4200 | 0.8345 | 0.8330 | 0.4167 | 0.8333 |
| 4 | 0.3342 | 0.3360 | 0.6753 | 0.6667 | 0.3333 | 0.6667 |
| 3 | 0.2475 | 0.2510 | 0.5001 | 0.4980 | 0.2500 | 0.5000 |
| 2 | 0.1628 | 0.1660 | 0.3290 | 0.3294 | 0.1667 | 0.3333 |
| 1 | 0.0798 | 0.0834 | 0.1612 | 0.1655 | 0.0833 | 0.1667 |
| 0 | 0 | | | 0 | 0 | 0 |

Notes: 1. Values in column "a" are based on the 1974 calibration of the integrating sphere.
2. Values in column "b" are based on the 1983 calibration of the integrating sphere.

## 5. Calibration of the Advanced Very High Resolution Radiometer

### 5.1 General

The factors influencing the visible and near-infrared radiances sensed by the AVHRR onboard the NOAA polar orbiting environmental satellite are:

a. the wavelength dependent atmospheric(absorption and scattering) and surface(reflection) processes;

and b. the wavelength dependent nature of the absorption, reflection and transmission properties of the various components of the optical train and of the silicon detector.

The procedure adopted for the pre-launch, laboratory calibration of Channels 1 and 2 of the AVHRR onboard NOAA-6 through NOAA-10 is directed towards the determination of the response of the entire optical subsystem, taking into account factors mentioned in (b), to changes in the ambient radiation field.

### 5.2 Normalized spectral response of Channels 1 and 2

The experimental set-up for the determination of the normalized spectral response- also referred to as normalized response- of Channels 1 and 2 is seen in Fig.5; it consists of a stable source(Nernst glower) of illumination, a 1/4-meter Jarrell-Ash Model 82-410 grating monochromator [resolving power: better than $3\times10^{-4}$μm at the wavelength of 0.313μm(second order spectrum) with 150μm slits ; dispersion: $3.3\times10^{-3}$μm/mm with the 1180 grooves/mm grating ), a beam-folding mirror and collimator assembly, a pyroelectric detector, and the AVHRR. The radiation

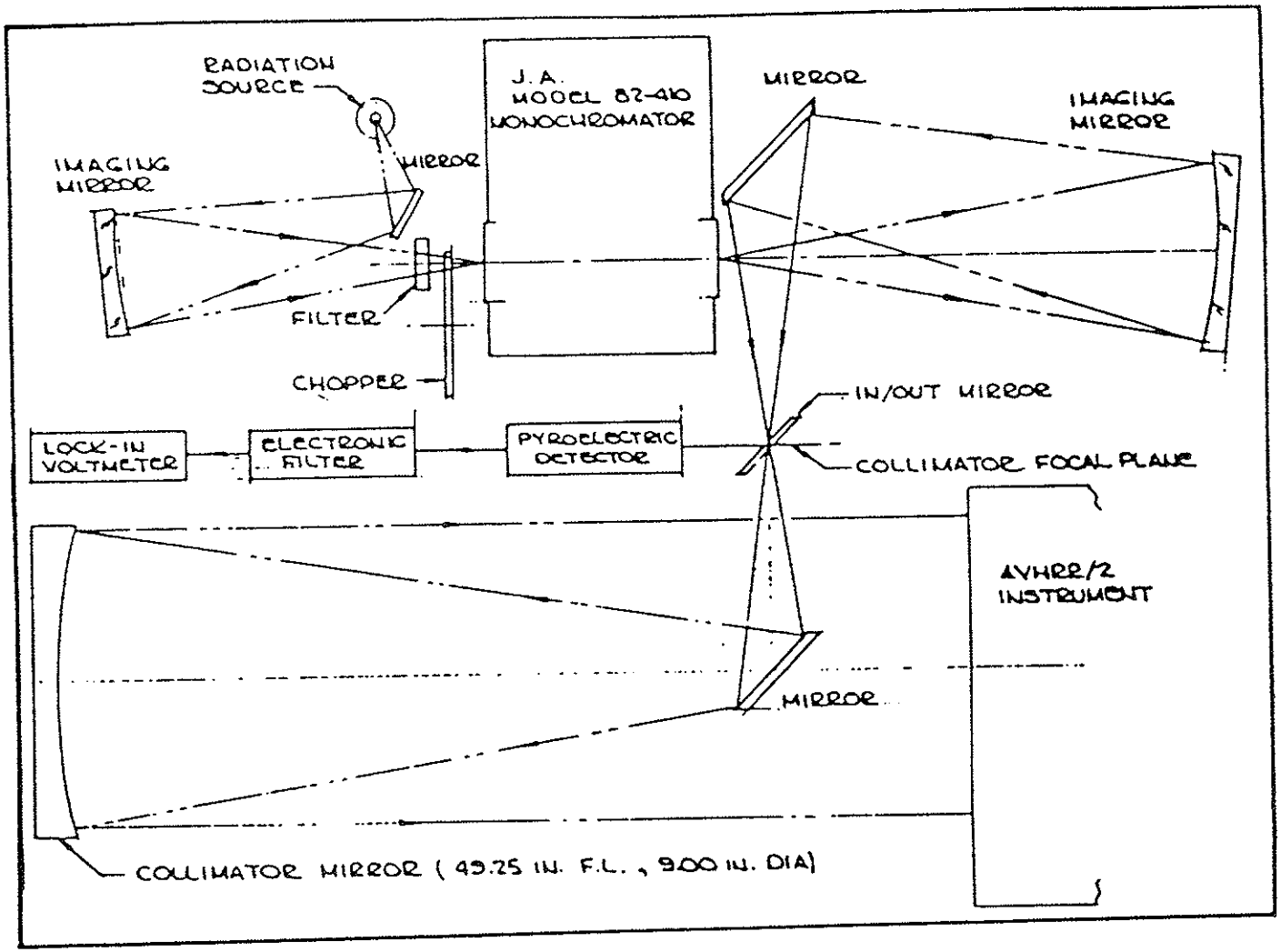


Figure 5. Experimental set-up for the determination of normalized spectral response

emerging from the exit slit of the monochromator is directed towards the pyroelectric detector when the "In-Out" mirror is in the light path; and towards the AVHRR when the "In-Out" mirror is removed from the light path.

The relative spectral radiance, in the form of voltages, of the Nernst glower, a standard temperature-controlled ceramic (zirconium oxide) rod which is heated to incandescence(1200$^{o}$C to 1700$^{o}$C) by passing an electric current through it, is measured at pre-determined wavelengths falling within the passband of each channel with the Jarell-Ash monochromator and pyroelectric detector. The radiation emerging from the exit slit of the monochromator is then directed towards the AVHRR by removing the "In-Out" mirror from the light path and the AVHRR signals are recorded at the same wavelengths.

The relative spectral response of the AVHRR at the wavelength $\lambda$ is then given by:

$$\tau_i = V_i/(V_r R_i) \qquad (12)$$

where $V_i$ : the AVHRR signal at the wavelength $\lambda$ ;

$V_r$ : the pyroelectric detector or reference signal at the wavelength $\lambda$ ;

and $R_i$ : the reflectance of the collimator mirror at the wavelength $\lambda$ ;

Similarly, the relative response of the AVHRR at the wavelength of peak or maximum response, $\lambda_p$, is given by

$$\tau_p = V_{ip}/(V_{rp} R_{ip}) \qquad (13)$$

where $V_{ip}$ : the AVHRR signal at the wavelength of peak response;

$V_{rp}$ : the pyroelectric detector or reference signal at the wavelength of peak response;

and $R_{lp}$ : the reflectance of the collimator mirror at the wavelength of peak response.

The normalized spectral response of the AVHRR at the wavelength $\lambda$ is then given by

$$\tau_\lambda = \tau_i / \tau_p \qquad (14)$$

We shall illustrate this method of calculating the normalized spectral response of the AVHRR by referring to the entries in Table 6 where we have shown data(ITT, 1980) obtained for Channel 1 of the AVHRR onboard NOAA-9. Let us consider the entries for the wavelength of 0.57μm(or 570nm as entered in the table). We notice that at this wavelength $V_l$ =990mv; $V_r$ =5.034mv; and $R_l$ =0.792. Also, the AVHRR is observed to have peak response at the wavelength of 0.680μm(or 680nm). The corresponding values of $V_{lp}$ , $V_{rp}$, and $R_{lp}$ are respectively 1976mv, 5.271mv and 0.764. Substitution of these numerical values in Eqns.12 and 13 will yield values of 248.3115 and 490.6825 for $\tau_i$ and $\tau_p$ respectively. Using these relative spectral response values in Eqn.14, we obtain a value of 0.5061 or 50.61% for the normalized spectral response of Channel 1 at the wavelength of 0.57μm.

It should be observed that the maximum normalized spectral response of 1 (or 100%) can occur at different wavelengths within the passband for different AVHRRs because of differences in the wavelength dependent characteristics of the various components of the optical train and of the responsivity of the detector(Fig.6)

Table 6. Laboratory determination of the normalized spectral response of Channel 1 of the AVHRR(FM 202) onboard NOAA-9

| WVLN | SIGNAL AMP. REF. | SIGNAL AMP. CH #1 | CH #1 REF. | MIRROR REFLECTANCE | RELATIVE SPECTRAL RESPONSE | NORMAL RESPONSE |
|---|---|---|---|---|---|---|
| 500 | 2.610mV | 0 | 0 | .810 | 0 | .0000 |
| 510 | 3.055 | 0 | 0 | .806 | 0 | .0000 |
| 520 | 3.386 | 0 | 0 | .802 | 0 | .0000 |
| 530 | 3.874 | 0 | 0 | .800 | 0 | .0000 |
| 540 | 4.202 | 1 | .2380 | .797 | .2986 | .0006 |
| 550 | 4.508 | 25 | 5.5457 | .796 | 6.9670 | .0142 |
| 560 | 4.772 | 383 | 80.2598 | .794 | 101.0829 | .2060 |
| 570 | 5.034 | 990 | 196.6627 | .792 | 248.3115 | .5061 |
| 580 | 5.184 | 1370 | 264.2747 | .790 | 334.5249 | .6818 |
| 590 | 5.359 | 1669 | 311.4387 | .788 | 395.2268 | .8055 |
| 600 | 5.545 | 1743 | 314.3372 | .786 | 399.9202 | .8150 |
| 610 | 5.603 | 1681 | 300.0178 | .784 | 382.6758 | .7800 |
| 620 | 5.646 | 1758 | 311.3709 | .781 | 398.6823 | .8125 |
| 630 | 5.692 | 1950 | 342.5861 | .779 | 439.7767 | .8963 |
| 640 | 5.651 | 1963 | 347.3721 | .777 | 447.0684 | .9111 |
| 650 | 5.715 | 1794 | 313.9108 | .774 | 405.5695 | .8265 |
| 660 | 5.616 | 1721 | 306.4459 | .772 | 396.9506 | .8090 |
| 670 | 5.495 | 1830 | 333.0300 | .768 | 433.6328 | .8837 |
| 680 | 5.271 | 1976 | 374.8814 | .764 | 490.6825 | 1.0000 |
| 690 | 5.160 | 1681 | 325.7752 | .762 | 427.5265 | .8713 |
| 700 | 5.171 | 907 | 175.4013 | .759 | 231.0952 | .4710 |
| 710 | 5.080 | 403 | 79.3307 | .756 | 104.9348 | .2139 |
| 720 | 4.978 | 180 | 36.1591 | .753 | 48.0201 | .0979 |
| 730 | 4.781 | 89 | 18.6154 | .748 | 24.8868 | .0507 |
| 740 | 4.579 | 49 | 10.7010 | .743 | 14.4025 | .0294 |
| 750 | 4.394 | 29 | 6.5999 | .738 | 8.9430 | .0182 |
| 760 | 10.40 | 50 | 4.8077 | .734 | 6.5500 | .0133 |
| 770 | 10.55 | 37 | 3.5071 | .732 | 4.7911 | .0098 |
| 780 | 10.60 | 28 | 2.6415 | .731 | 3.6136 | .0074 |
| 790 | 10.75 | 24 | 2.2326 | .726 | 3.0751 | .0063 |
| 800 | 10.80 | 23 | 2.1296 | .722 | 2.9496 | .0060 |

Source: Alignment and Calibration Data Book, AVHRR/2, SN 202 (ITT, 1980)

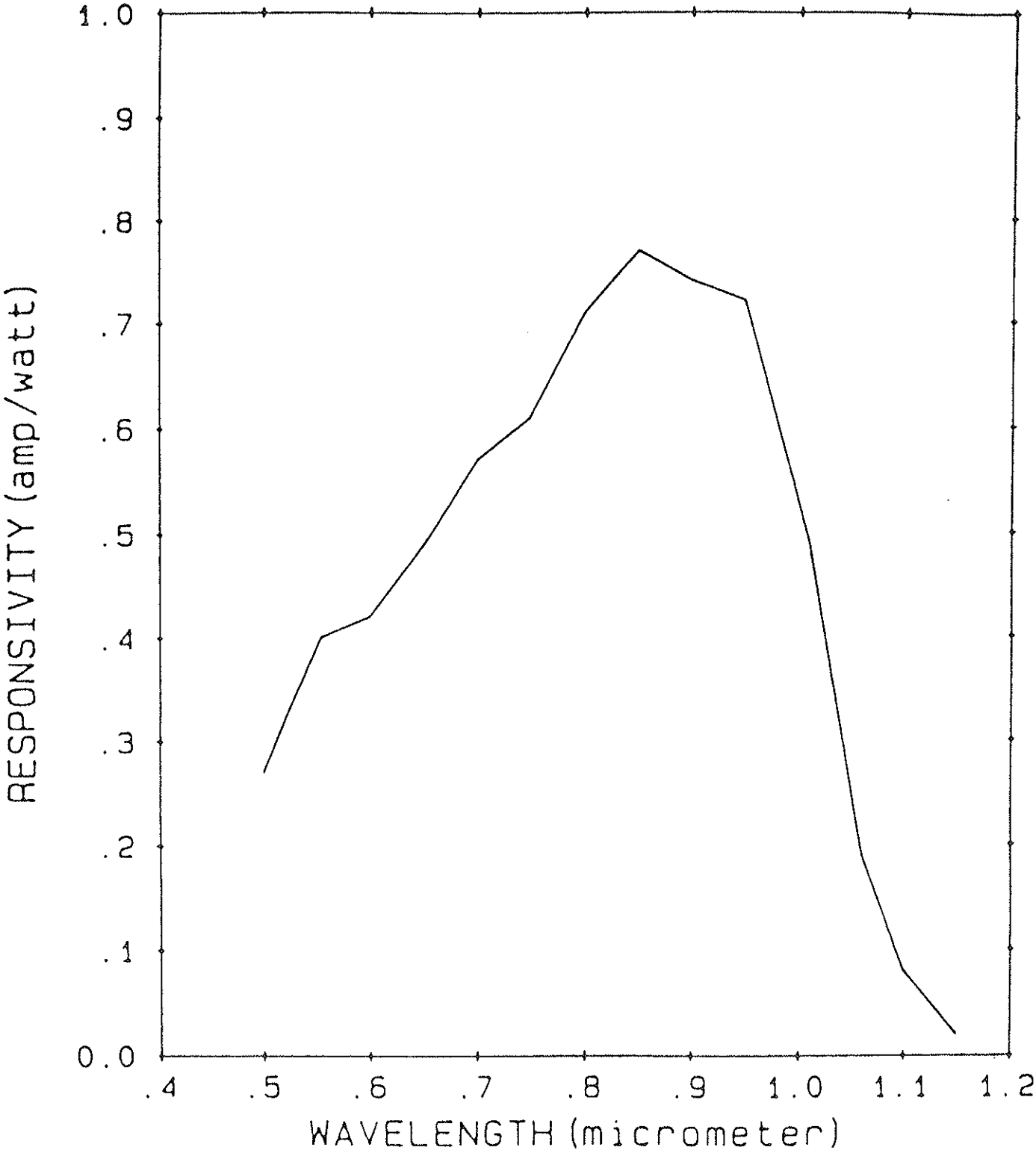


Figure 6. Typical spectral responsivity of the silicon detector at room temperature

mentioned earlier; the shape of the normalized response curves could also be different; these features are illustrated in Figs. 7-11. The small but finite off-band response, at wavelengths longer than 0.8um, in Channel 1 of the AVHRR onboard NOAA-8(Fig.9) contributes about 2% of the various filtered radiances and irradiances, and affects the equivalent width of the channel to the same extent; the mean wavelength is affected to a smaller degree. Similar, off-band responses in Channel 1 of the AVHRR onboard NOAA-6(Fig.7) and in Channel 2 of the AVHRR onboard NOAA-7(Fig.8) have much smaller effects.

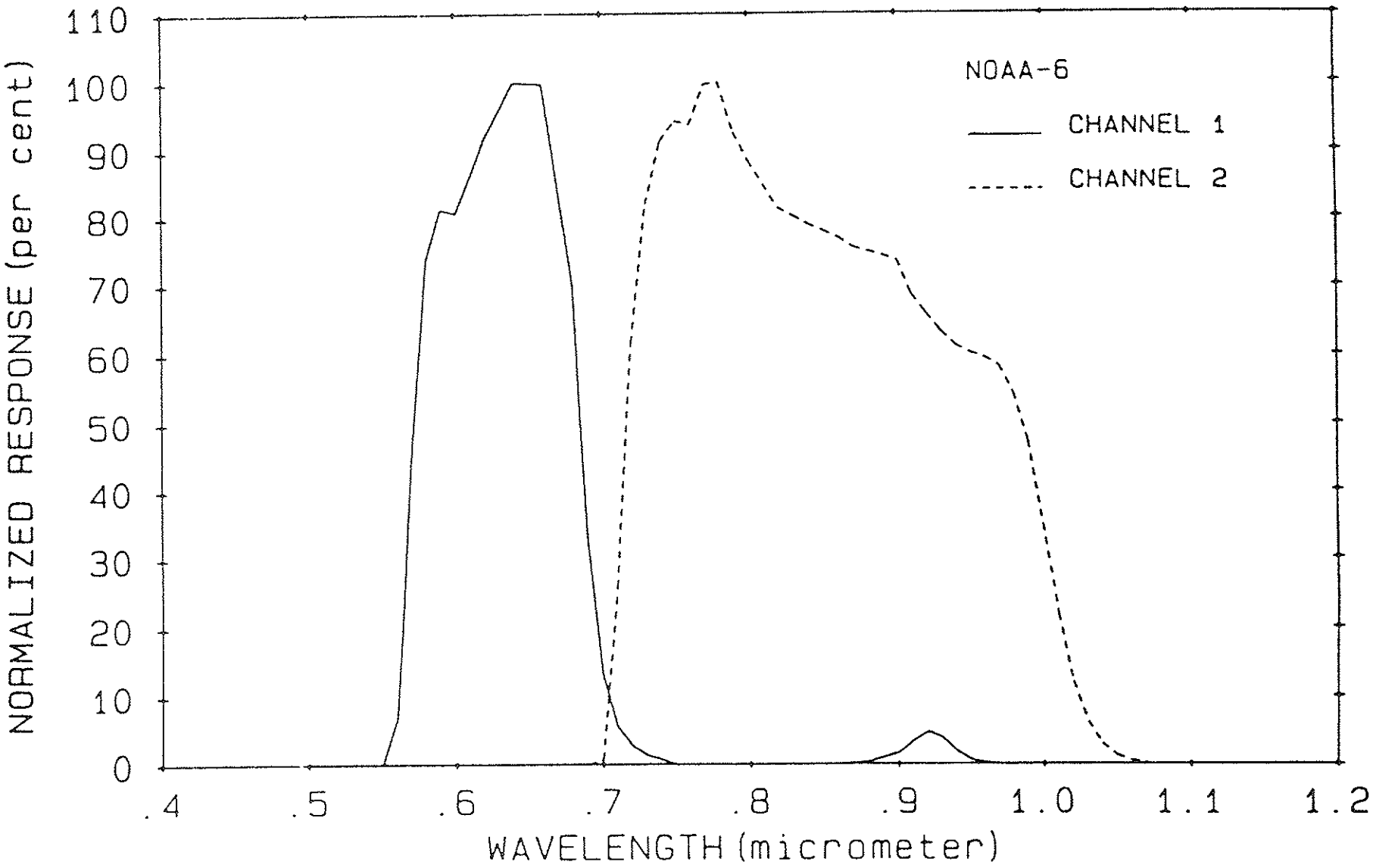


Figure 7. Normalized spectral response of the AVHRR(FM 103) onboard NOAA-6

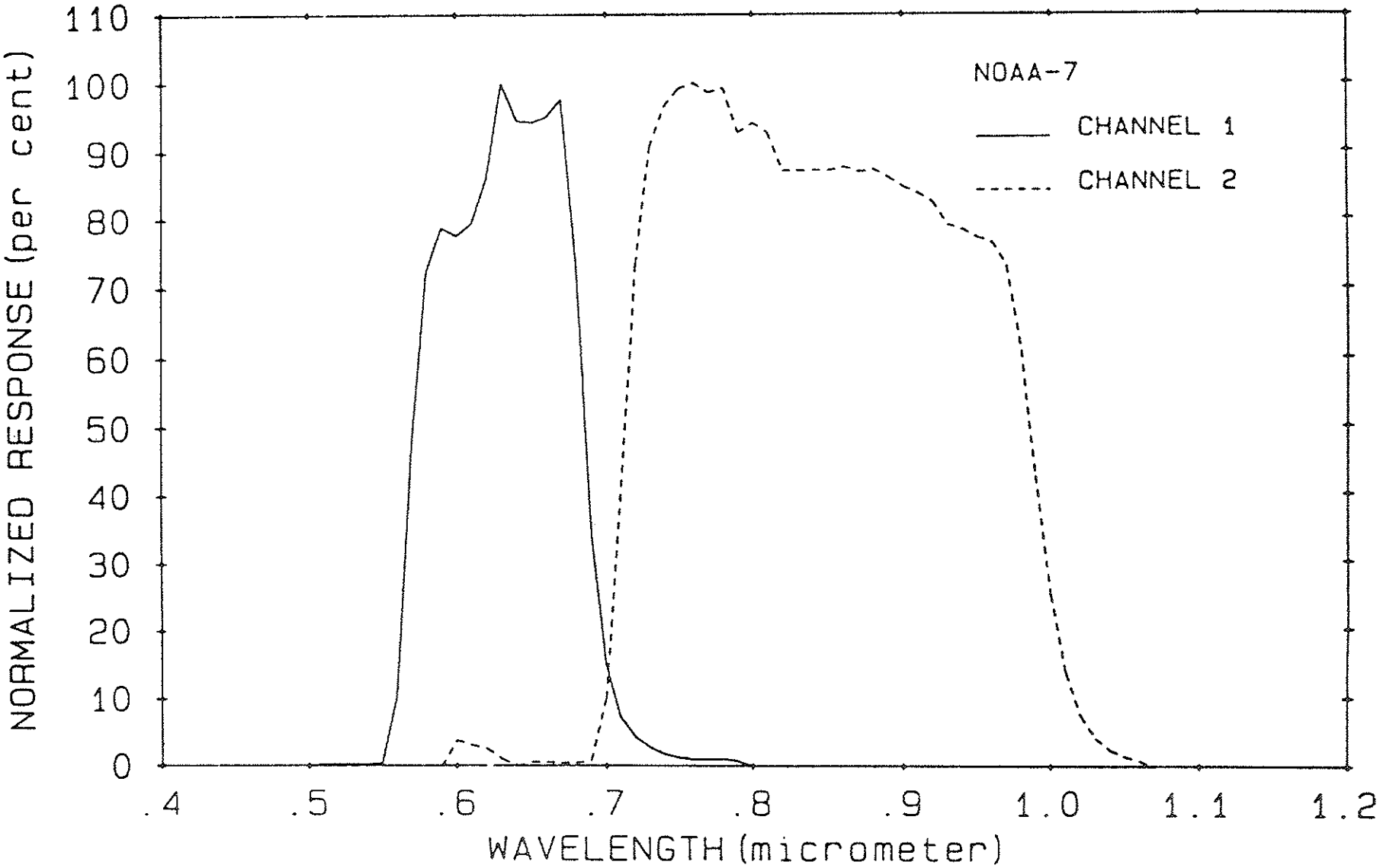


Figure 8. Normalized spectral response of the AVHRR(FM 201) onboard NOAA-7

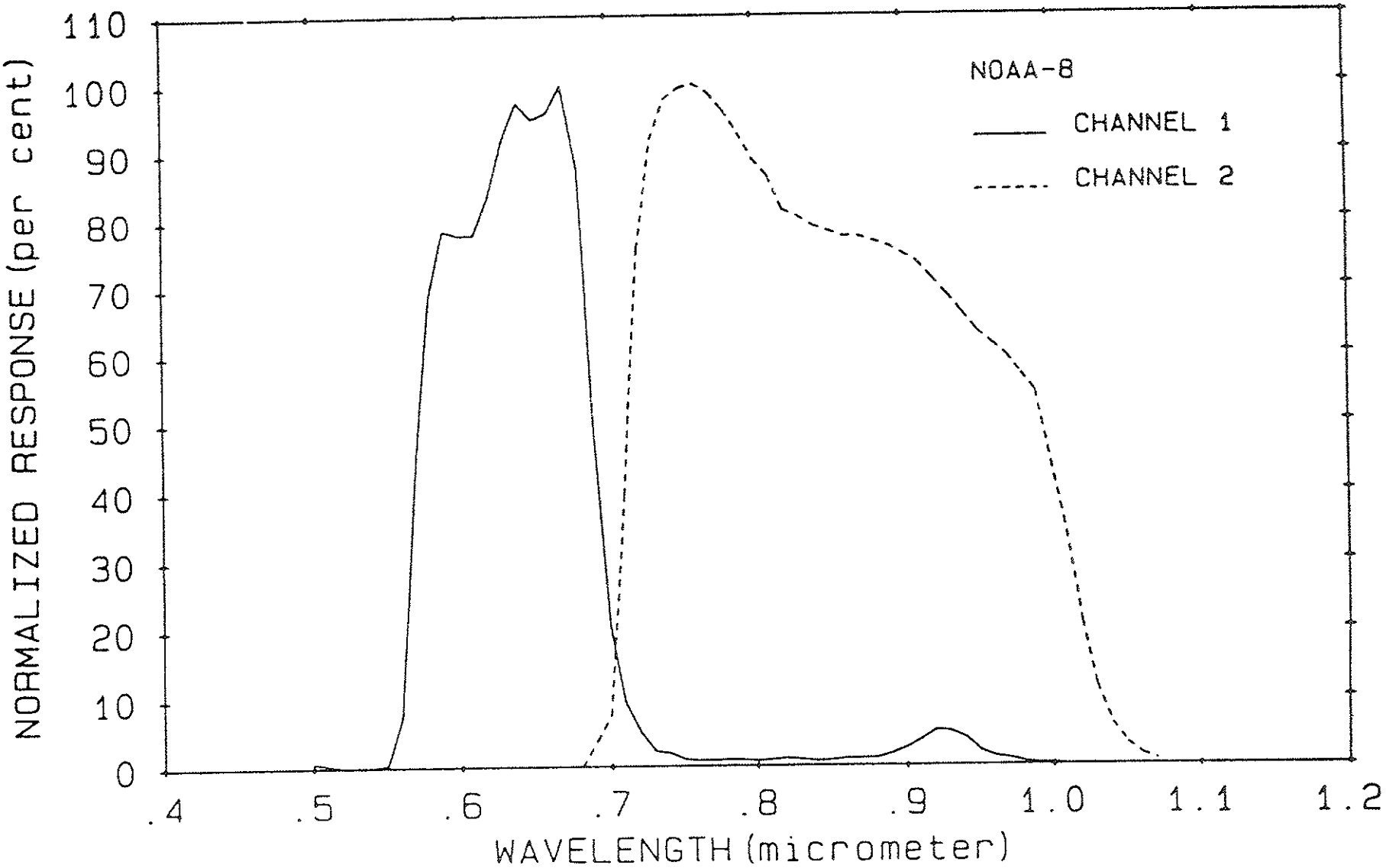


Figure 9. Normalized spectral response of the AVHRR(FM 102) onboard NOAA-8

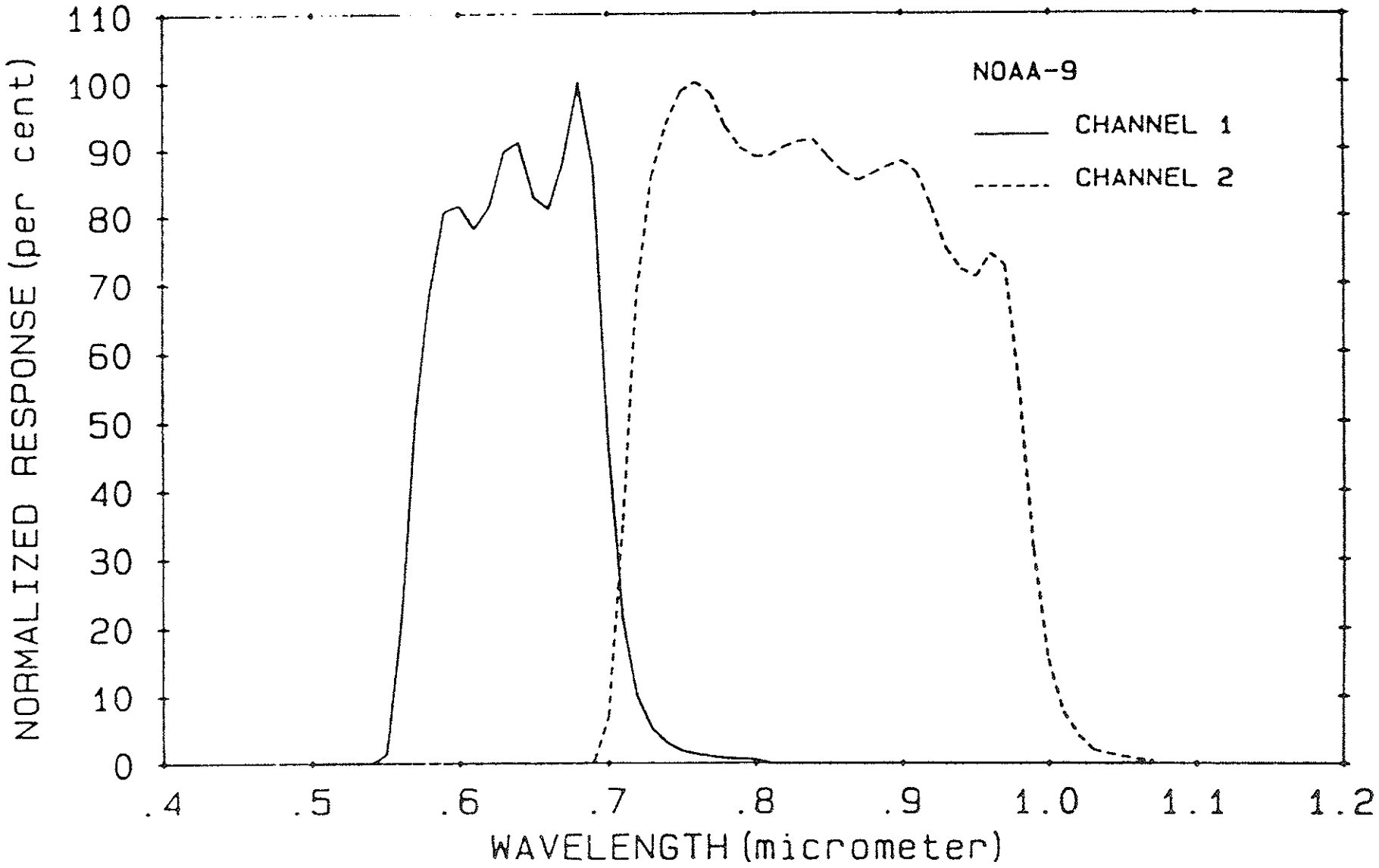


Figure 10. Normalized spectral response of the AVHRR(FM 202) onboard NOAA-9

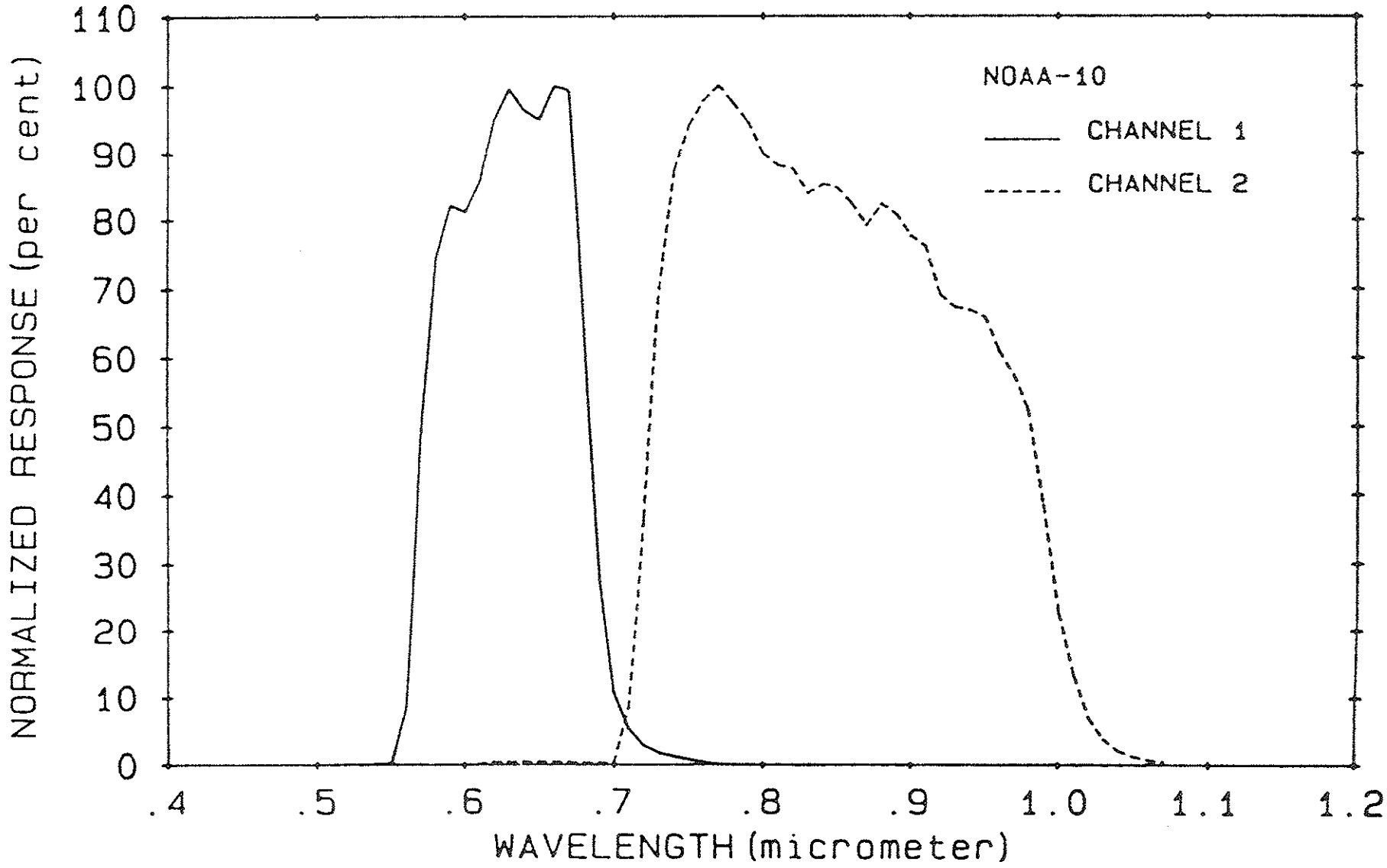


Figure 11. Normalized spectral response of the AVHRR(FM 101) onboard NOAA-10

## 5.3 Determination of the reflectance factor of the integrating sphere

The experimental set-up for the determination of the reflectance factor of the integrating sphere in the laboratory is seen in Fig.12. It consists of the integrating sphere, the AVHRR, the space clamp target, the AVHRR Bench Control Unit(BCU) computer and associated electronics. A very detailed procedure has been established by ITT Aerospace/Optical Division for the operation of the integrating sphere, with special reference to the manner and order in which the twelve matched quartz-halogen lamps should be switched on and off. The space clamp target- a cubic (~3'on the side), honeycomb structure blackened on the inside- is used to simulate space-view conditions for the AVHRR.

The experiment is started with the illumination of the sphere at its highest,i.e., with 12 lamps on for Channel 1 and, for reasons mentioned earlier, with 6 lamps on for Channel 2. The AVHRR is directed to view the 12-inch aperture of the integrating sphere and 3600 measurements are made of the AVHRR signal, in volts, by the BCU computer; the mean and standard deviation of these measurements are then calculated and recorded as the uncorrected AVHRR signal and noise, respectively; the corresponding counts on a 10-bit scale are calculated by multiplying these AVHRR signals, expressed in millivolts, by 0.160 and rounding off the product to the nearest integer. The AVHRR is then directed towards the space clamp target and the corresponding space clamp signal and noise are recorded. This procedure is

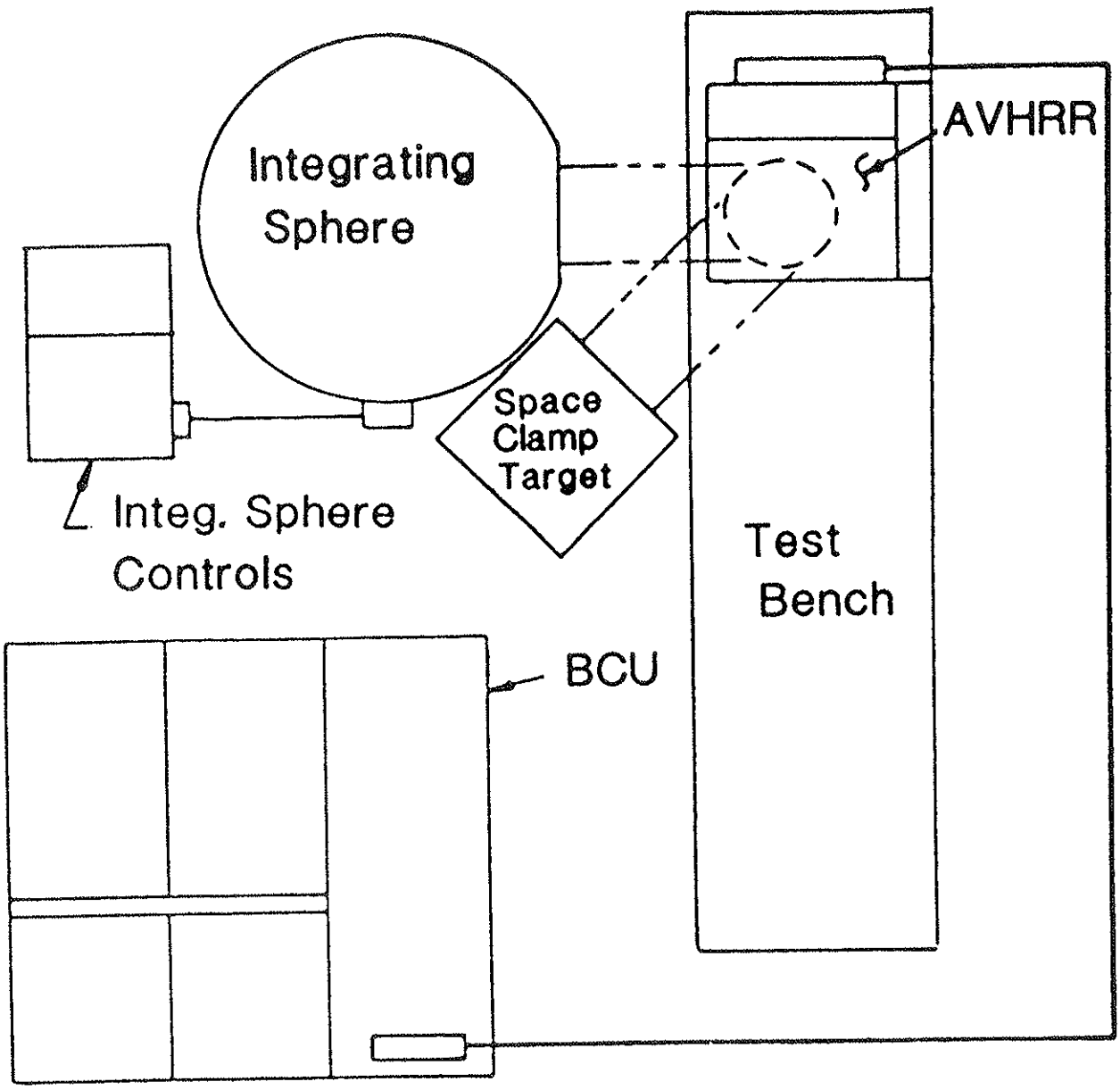


Figure 12. Experimental set-up for the radiance calibration of AVHRR Channels 1 and 2

repeated, switching off one lamp at a time in a predetermined order - thereby varying the integrating sphere radiance in a known, step-wise manner- until all the lamps have been switched off. It is observed that the AVHRR signal when it views the integrating sphere with all the lamps switched off is very close to the space clamp signal, as it should be. This zero level signal is then subtracted from the signals measured at various levels of illumination of the integrating sphere and the result recorded as the corrected signal. The ratio of the corrected AVHRR signal when the radiometer is viewing the integrating sphere illuminated with n lamps(integer $n \leq 12$ for Channel 1; $\leq 6$ for Channel 2) to the corrected AVHRR signal when the radiometer is viewing the integrating sphere illuminated with 12 or 6 lamps as the case may be is calculated; the degree of correspondence between this ratio and the sphere ratio(see Section 4.3) is a measure of the linearity of response of the AVHRR over its dynamic range, assuming that the integrating sphere radiance varies linearly, over the spectral region of interest, with the number of lamps that have been switched on and that its spectral distribution is not affected by the number of lamps that are on. Experimental evidence indicates that the response of the AVHRR may be considered linear for all practical purposes. However, the purpose of the pre-launch calibration of the AVHRRs onboard NOAA-6 through NOAA-10 has been to relate the uncorrected AVHRR signals, expressed in counts, to the reflectance factor of the integrating sphere as the number of lamps is changed from 12 to 0 for Channel 1

and from 6 to 0 for Channel 2 in steps of 1.

We have illustrated in Tables 7 and 8 the procedure adopted in the laboratory to calculate the reflectance factor of the integrating sphere when all the 12 lamps are on, using data for Channels 1 and 2 of the AVHRR(SN 202) onboard NOAA-9; the passbands of the two channels have been divided into 6 intervals; the average values of the normalized response, the sphere irradiance and the solar irradiance(Thekaekara 1974) were then calculated over these intervals and used in the computation of the integrating sphere and solar output; the reflectance factor (or albedo) is then given by the ratio of the total sphere output to the total solar output; however, in the case of Channel 2, since we have computed the total sphere output corresponding to illumination of the integrating sphere with 12 lamps, we have to multiply it by the sphere ratio corresponding to 6 lamps-0.5040(Table 5) for the 1983 calibration- before calculating the reflectance factor for reasons mentioned earlier(Section 4.2).

It should be noted that the choice of the number of spectral intervals into which the passband of a channel is divided in the calculation of the reflectance factor of the integrating sphere is purely arbitrary; our work(vide Table 13) has shown that the calculated reflectance factors vary by about a percent as the number of spectral intervals is changed from 6 to 20 or more, provided the average values of the normalized response function of the channel and of the various irradiances have been properly computed.

Table.7. Reflectance factor of Channel 1(AVHRR FM 202;NOAA-9)

| Spectral interval | Relative response | Sphere irradiance | Solar irradiance | Sphere output | Solar output |
|---|---|---|---|---|---|
| 0.55-0.60 | 0.505 | 966.1 | 1702.2 | 24.39 | 42.98 |
| 0.60-0.65 | 0.840 | 1225.2 | 1588.0 | 51.46 | 66.70 |
| 0.65-0.68 | 0.879 | 1419.4 | 1470.0 | 37.43 | 38.76 |
| 0.68-0.70 | 0.781 | 1538.7 | 1399.3 | 24.03 | 21.86 |
| 0.70-0.75 | 0.147 | 1685.5 | 1302.0 | 12.39 | 9.57 |
| 0.75-0.80 | 0.010 | 1844.1 | 1172.2 | 0.92 | 0.59 |
| | | | Sum: | 150.62 | 180.46 |

$$\text{Reflectance factor or albedo: } \frac{\text{Total sphere output}}{\text{Total solar output}}$$

: 150.62/180.46= 0.8346 or 83.46%

Notes: Wavelengths are in units of micrometer.

Irradiances are in units of $Wm^{-2}\mu m^{-1}$
Integrating and sphere outputs are in units of $Wm^{-2}$
Solar output: product of the width of the spectral interval, the relative response, and the solar irradiance.
Sphere output: product of the width of the spectral interval, the relative response and the sphere irradiance.

Table.8. Reflectance factor of Channel 2(AVHRR SN 202;NOAA-9)

| Spectral interval | Relative response | Sphere irradiance | Solar irradiance | Sphere output | Solar output |
|---|---|---|---|---|---|
| 0.69-0.72 | 0.224 | 1604.3 | 1357.3 | 10.78 | 9.12 |
| 0.72-0.78 | 0.912 | 1770.9 | 1236.3 | 96.90 | 67.65 |
| 0.78-0.83 | 0.904 | 1894.4 | 1097.2 | 85.62 | 49.59 |
| 0.83-0.88 | 0.881 | 1917.0 | 980.0 | 84.44 | 43.17 |
| 0.88-0.94 | 0.823 | 1918.7 | 882.7 | 94.74 | 43.59 |
| 0.94-1.07 | 0.292 | 1876.6 | 742.7 | 71.23 | 28.19 |
| | | | Sum: | 443.71 | 241.31 |

The sphere output corresponds to illumination with 12 lamps; however, only 6 lamps are on when Channel 2 is calibrated; thus, the sphere output should be multiplied by the appropriate sphere ratio(Table 5; 1983) which, in this case, is 0.5040.

$$\text{Reflectance factor or albedo: } \frac{0.5040 * \text{Total sphere output}}{\text{Total solar output}}$$

: 223.63/241.31= 0.9267 or 92.67%

Notes: Wavelengths are in units of micrometer.

Irradiances are in units of $Wm^{-2}\mu m^{-1}$
Integrating and sphere outputs are in units of $Wm^{-2}$.
Solar output: product of the width of the spectral interval, the relative response, and the solar irradiance.
Sphere output: product of the width of the spectral interval, the relative response and the sphere irradiance.

We shall now illustrate the regression of the integrating sphere reflectance factor on the AVHRR digital signal, using the data(ITT, 1980) in Table 9 where we have shown the measurements obtained with Channels 1 and 2 of the AVHRR(SN 202) onboard NOAA-9. The entries in the 'albedo' column are obtained by multiplying the reflectance factor of the integrating sphere at full illumination(12 lamps for Channel 1; 6 lamps for Channel 2) by the appropriate sphere ratios listed in Table 5; for example, the reflectance factor of 47.82% in Channel 1 when the sphere is illuminated with 7 lamps is obtained by multiplying the 'albedo' of 82.43% at the level of highest illumination by the sphere ratio of 0.5801. The corresponding AVHRR digital signals, entered in the 'CNTS'column, are obtained, as was mentioned earlier, by multiplying the AVHRR signals in millivolts listed in the 'SIGNAL MV' column by 0.160 and rounding off the product to the nearest integer. There are 13 pairs of 'albedo-counts' data, including measurements made when the integrating sphere is not illuminated( number of lamps: 0) for Channel 1; and 7 for Channel 2. Simple regression of 'albedo' on counts yields the following regression coefficients:

Channel 1; slope= 0.1063(%/count), intercept=-3.8404(%)

Channel 2; slope= 0.1073(%/count), intercept=-3.8448(%)

These values differ slightly from the operational values given in Table 14.

The dependence of 'albedo' on counts measured in the above channels is seen in Fig.13.

Table 9. Data for the development of the regression relationship between the reflectance factor(albedo) of the integrating sphere and the AVHRR signals(FM 202; NOAA-9)

| CHANNEL 1 | | | | | | | CHANNEL #2 | | | | | |
|---|---|---|---|---|---|---|---|---|---|---|---|---|
| NO. LAMPS | % ALBEDO | SIGNAL MV | CNTS. | STD.DEV MV | SPACE SIGNAL MV | SPACE STD.DEV MV | % ALBEDO | SIGNAL MV | CNTS. | STD.DEV MV | SPACE SIGNAL MV | SPACE STD.DEV MV |
| 12 | 82.43 | 5075.98 | 812 | 2.402 | 244.05 | 1.939 | | | | | | |
| 11 | 75.46 | 4656.08 | 745 | 1.284 | 243.93 | 2.079 | | | | | | |
| 10 | 68.70 | 4268.78 | 683 | 1.687 | 244.08 | 2.308 | | | | | | |
| 9 | 61.86 | 3859.47 | 618 | 2.953 | 243.93 | 2.070 | | | | | | |
| 8 | 54.79 | 3443.06 | 551 | 1.905 | 243.99 | 2.091 | | | | | | |
| 7 | 47.82 | 3030.73 | 485 | 1.802 | 243.87 | 2.096 | | | | | | |
| 6 | 40.79 | 2630.89 | 421 | 1.600 | 243.85 | 1.980 | 96.72 | 5862.49 | 940 | 2.106 | 250.25 | 1.940 |
| 5 | 34.04 | 2234.16 | 357 | 2.920 | 243.70 | 2.112 | 80.71 | 4930.74 | 789 | 1.749 | 250.14 | 1.636 |
| 4 | 27.55 | 1837.61 | 294 | 1.311 | 243.74 | 2.033 | 65.31 | 3998.90 | 640 | 2.800 | 250.55 | 2.145 |
| 3 | 20.40 | 1417.18 | 227 | 2.555 | 243.83 | 2.175 | 48.32 | 3024.98 | 484 | 1.973 | 250.15 | 1.714 |
| 2 | 13.42 | 1009.12 | 161 | 2.838 | 243.84 | 2.088 | 31.82 | 2074.18 | 332 | 1.871 | 250.33 | 1.948 |
| 1 | 6.58 | 604.19 | 97 | 2.783 | 243.76 | 2.073 | 15.60 | 1117.46 | 179 | 2.623 | 250.31 | 1.922 |
| 0 | 0 | 244.97 | 39 | 2.545 | 243.74 | 2.117 | 0 | 250.01 | 40 | 1.735 | 250.30 | 2.019 |

Source: Alignment and Calibration Date Book, AVHRR/2, SN 202 (ITT, 1980)

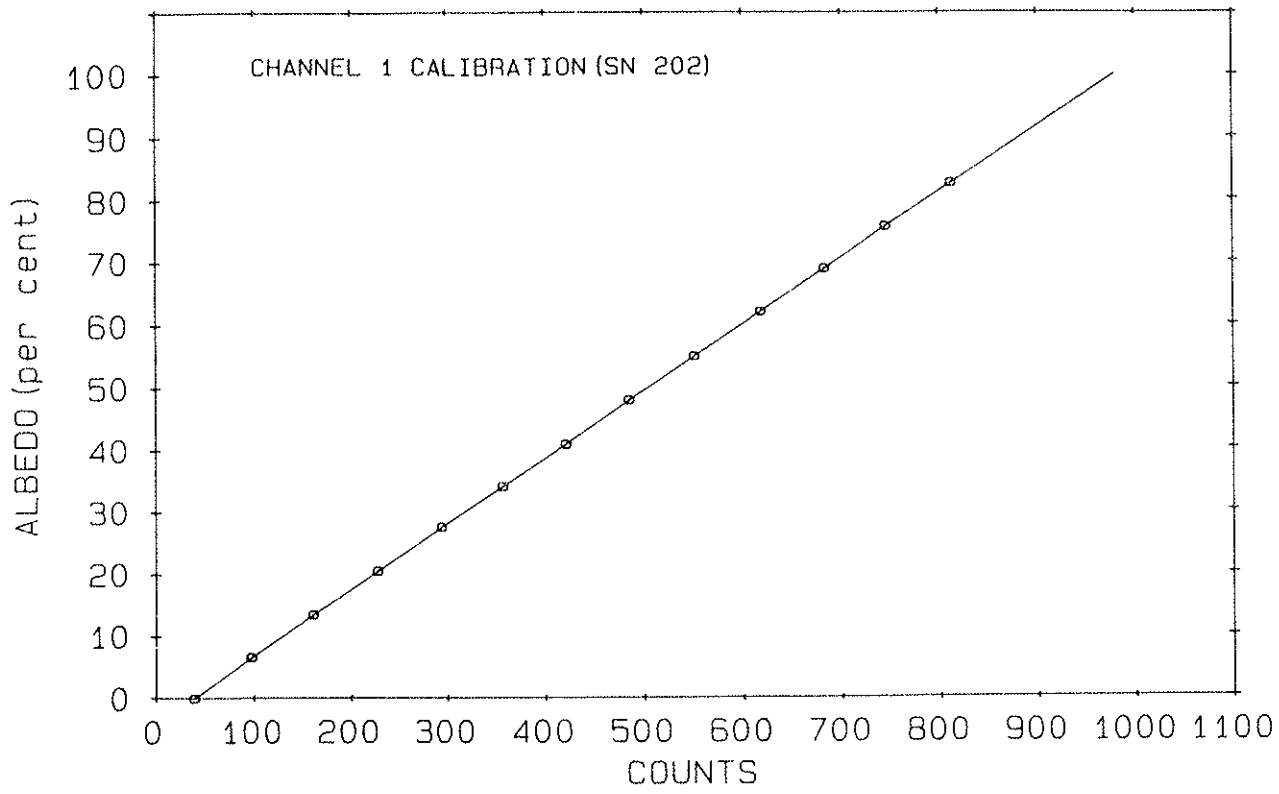


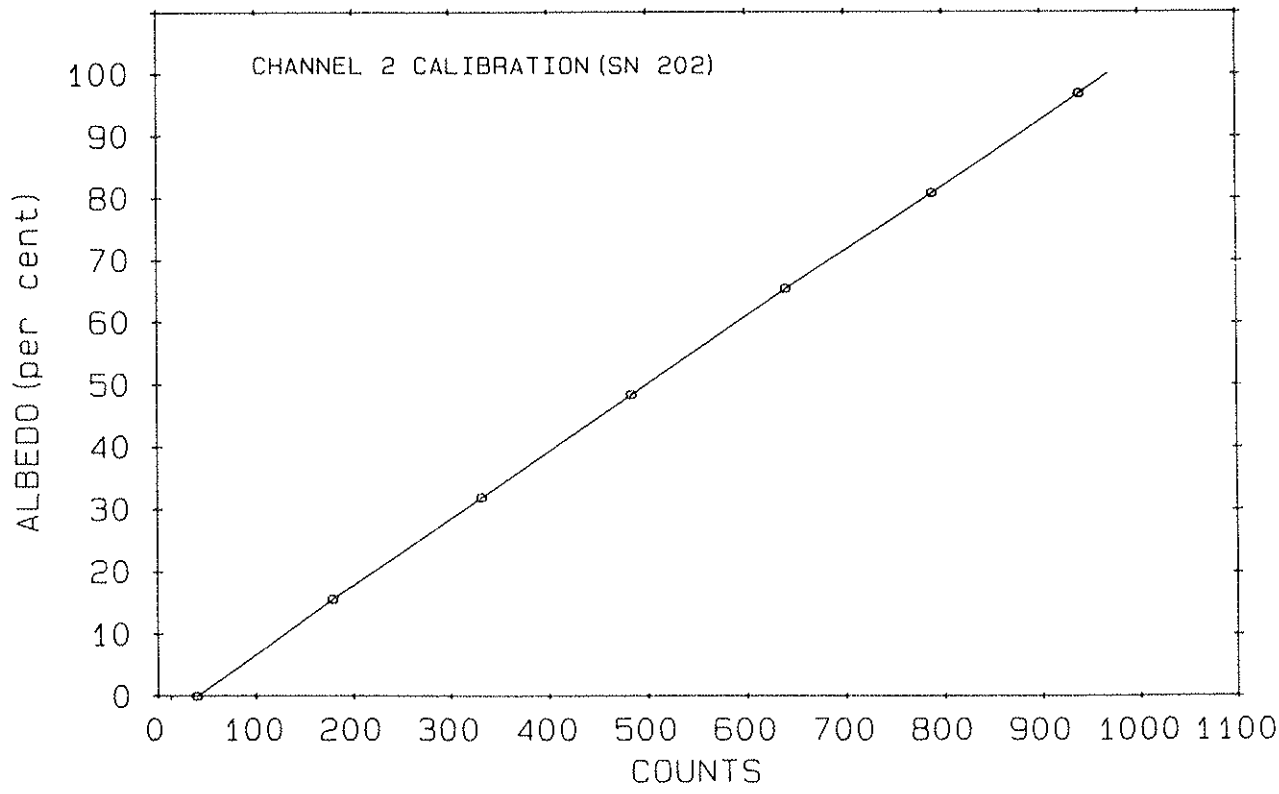


Figure 13. Regression of albedo(reflectance factor) on AVHRR digital signals

## 6. Results and discussion

### 6.1 General

We shall now examine the dependence of the filtered solar irradiance and, consequently, of the reflectance factor of the integrating sphere, on the extraterrestrial solar spectral irradiance data used in the laboratory calibration; it is apparent that these dependencies will affect the regression relationship between the reflectance factor and the AVHRR digital signals.

### 6.2 Filtered solar irradiance

We have shown the filtered solar irradiance in the two channels of the AVHRRs onboard NOAA-6 through NOAA-10 corresponding to the Air Force(1965), Thekaekara(1974) and Neckel and Labs(1984) spectral solar irradiance data in Table 10. The Air Force(1965) data yield the highest value for the filtered solar irradiance in Channel 1, followed by the Neckel and Labs(1984) and Thekaekara(1974) data, in that order; however, in Channel 2, the Neckel and Labs(1984) data yield the highest value for the filtered solar irradiance, followed by the Air Force(1965) and Thekaekara(1974) data. The difference between the maximum and minimum filtered solar irradiance values is about 8.3% of the minimum value in Channel 1 and about 2.5% in Channel 2; on the other hand, the mean wavelength is hardly affected by the changes in the spectral solar irradiance.

In a recent review of the calibration of satellite radiometers, Price(1987) has published values of the 'bandwidth' and 'equivalent solar radiance', $w$ and $F/\pi w$ respectively in our

Table 10. Filtered solar irradiance, effective wavelength, and the equivalent width of AVHRR Channels 1 and 2

| Satellite | Channel 1 | | | | | | | Channel 2 | | | | | | |
|---|---|---|---|---|---|---|---|---|---|---|---|---|---|---|
| | $w(\mu m)$ | $F(Wm^{-2})$ | | | $\bar{\lambda}(\mu m)$ | | | $w(\mu m)$ | $F(Wm^{-2})$ | | | $\bar{\lambda}(\mu m)$ | | |
| | | a | b | c | a | b | c | | a | b | c | a | b | c |
| NOAA-6 | 0.109 | 183.8 | 179.0 | 169.6 | 0.631 | 0.631 | 0.632 | 0.223 | 230.4 | 233.7 | 228.0 | 0.832 | 0.834 | 0.834 |
| NOAA-7 | 0.108 | 182.4 | 177.5 | 168.2 | 0.630 | 0.630 | 0.630 | 0.249 | 258.2 | 261.9 | 255.3 | 0.830 | 0.832 | 0.832 |
| NOAA-8 | 0.113 | 188.2 | 183.4 | 174.0 | 0.637 | 0.638 | 0.638 | 0.230 | 239.6 | 242.8 | 236.8 | 0.828 | 0.830 | 0.830 |
| NOAA-9 | 0.117 | 196.4 | 191.3 | 181.5 | 0.635 | 0.635 | 0.636 | 0.239 | 248.1 | 251.8 | 245.5 | 0.831 | 0.833 | 0.833 |
| NOAA-10 | 0.108 | 183.8 | 178.8 | 169.4 | 0.628 | 0.628 | 0.628 | 0.222 | 228.0 | 231.5 | 225.7 | 0.834 | 0.836 | 0.836 |

Notes:
1. Using the Air Force(1965) solar spectral irradiance data.
2. Using the Neckel and Labs(1984) solar spectral irradiance data.
3. Using the Thekaekara(1974) solar spectral irradiance data.

notation, for the different AVHRRs; the 'equivalent solar radiance' values are based on the Thekaekara(1974) spectral solar irradiance data. We have compared his computations with our results in Table 11. We see that there is very good correspondence between the two sets of values.

Using the filtered integrating sphere irradiances from Table 12, based on the 1983 calibration of the sphere, and the data shown in Table 10, we have computed the reflectance factor- the ratio of the filtered integrating sphere irradiance to the filtered solar irradiance- of the integrating sphere when it is illuminated with 12 lamps for Channel 1 and with 6 for Channel 2, for the Air Force(1965), Thekaekara(1974) and Neckel and Labs(1984) spectral solar irradiance data; these are shown in Table 13. It is apparent that the sense of variation of the reflectance factor of the integrating sphere with changes in the spectral solar irradiance is opposed to that of the filtered solar irradiance. We have also shown in column 'd' the reflectance factors that have been used to derive the currently operational regression relationships between the reflectance factor and AVHRR digital signals; apparently, these are also based on the Thekaekara(1974) spectral solar irradiance data. We see that the magnitude of the difference between the two sets of values of the integrating sphere reflectance factor calculated using the Thekaekara(1974) data ranges from 0.1%(Channel 1 of the AVHRR onboard NOAA-6) to 4.9%(Channel 2 of the AVHRR onboard NOAA-9). Part of these discrepancies could perhaps be attributed to the

Table 11. Comparison of w and $F/\pi w$ parameters

| | w(μm) | | $F/\pi w$ ($Wm^{-2}\mu m^{-1}sr^{-1}$) | |
|---|---|---|---|---|
| Channel | Price(1987) | Present work | Price (1987) | Present work |
| N6C1 | 0.108 | 0.109 | 499.0 | 495.4 |
| N6C2 | 0.223 | 0.223 | 325.0 | 325.7 |
| N7C1 | 0.108 | 0.108 | 498.0 | 497.5 |
| N7C2 | 0.248 | 0.249 | 325.0 | 326.6 |
| N8C1 | 0.113 | 0.113 | 488.0 | 488.4 |
| N8C2 | 0.229 | 0.230 | 327.0 | 328.0 |
| N9C1 | 0.117 | 0.117 | 492.0 | 492.0 |
| N9C2 | 0.240 | 0.239 | 326.0 | 326.3 |
| N10C1 | 0.108 | 0.108 | 499.0 | 499.3 |
| N10C2 | 0.222 | 0.222 | 323.0 | 323.6 |

Notes: 1. Channel identification NxCy; x: satellite y: channel
2. Price's values for NOAA-9 and NOAA-10 are pre-publication data.

Table 12. Filtered integrating sphere irradiance at maximum illumination

| Channel | Irradiance($Wm^{-2}$) |
|---|---|
| N6C1 | 137.8 |
| N6C2 | 209.9 |
| N7C1 | 135.7 |
| N7C2 | 233.9 |
| N8C1 | 146.8 |
| N8C2 | 215.8 |
| N9C1 | 151.2 |
| N9C2 | 225.4 |
| N10C1 | 135.0 |
| N10C2 | 209.4 |

Notes:
1. Channel identification; see Table 11.
2. Channel 1 values are based upon illumination of the integrating sphere with 12 lamps(1983 calibration).
3. Channel 2 values were obtained by multiplying the sphere irradiance corresponding to illumination with 12 lamps by the appropriate sphere ratio of 0.5040 for 6 lamps(Table 5) based on the 1983 calibration of the sphere.

Table 13. Reflectance factor(albedo) of the integrating sphere

| Channel | Reflectance factor(%) a | b | c | d |
|---|---|---|---|---|
| N6C1 | 75.0 | 77.0 | 81.2 | 81.30* |
| N6C2 | 91.1 | 89.8 | 92.1 | 92.50* |
| N7C1 | 74.4 | 76.4 | 80.6 | 79.10+ |
| N7C2 | 90.6 | 89.3 | 91.6 | 93.13+ |
| N8C1 | 78.0 | 80.0 | 84.3 | 81.50* |
| N8C2 | 90.1 | 88.9 | 91.1 | 92.50* |
| N9C1 | 77.0 | 79.1 | 83.3 | 82.43+ |
| N9C2 | 90.9 | 89.5 | 91.8 | 96.72+ |
| N10C1 | 73.4 | 75.5 | 79.7 | 81.20* |
| N10C2 | 91.9 | 90.5 | 92.8 | 92.50* |

Notes: 1. Channel identification; see Table 11.
2. Entries in columns a, b, and c are based on the 1983 calibration of the integrating sphere.
   a. Using the Air Force(1965) solar spectral irradiance data.
   b. Using the Neckel and Labs(1984) solar spectral irradiance data.
   c. Using the Thekaekara(1974) solar spectral irradiance data.
   d. Values based on the 1974 calibration of the integrating sphere, using the Thekaekara(1974) solar spectral irradiance data, taken from the appropriate editions of the "Alignment and Calibration Data Book" published by ITT Aerospace/Optical Division.
   *: read from graphs
   +: tabulated values

fact that the values in column 'd' are based on the 1974 calibration of the integrating sphere ; to the differences in the manner in which the average values of the normalized spectral response functions that have been used in the calculation of the filtered solar and integrating sphere irradiances have been computed; to the differences in the widths of the spectral intervals used in the numerical quadrature; and to the fact that some of the entries in column 'd' have been read from graphs.

6.3 The operational regression relationships

We have shown in Table 14 the slopes and intercepts of the regression relationships that have been used on an operational basis; they are taken from the appendices to NOAA Technical Memorandum 107, "Data Extraction and Calibration of TIROS -N/NOAA Radiometers"(Lauritson et al.,1979). It has been suggested that the similarities of slopes and intercepts for the five instruments would indicate that the degradation of the channel response or of the integrating sphere could be small over the period of 2-3 years(Table 15) over which the calibrations have been performed.

It should be noted that the slopes and intercepts would change by amounts proportional to the relative differences amongst the integrating sphere reflectance factors shown in Table 13 if spectral solar irradiance data different from the Thekaekara(1974) data are used.

7. Concluding remarks

As we have stated earlier, this report is a compilation of information on the pre-launch calibration of Channels 1 and 2 of

Table 14. Regression of the reflectance factor on AVHRR counts

| Satellite | Channel 1 | | Channel 2 | |
|---|---|---|---|---|
| | Slope(b) | Intercept(a) | Slope(b) | Intercept(a) |
| NOAA-6 | 0.1071 | -4.1136 | 0.1058 | -3.4539 |
| NOAA-7 | 0.1068 | -3.4400 | 0.1069 | -3.4880 |
| NOAA-8 | 0.1060 | -4.1619 | 0.1060 | -4.1492 |
| NOAA-9 | 0.1063 | -3.8464 | 0.1075 | -3.8770 |
| NOAA-10 | 0.1059 | -3.5279 | 0.1061 | -3.4767 |

Notes: 1. Reflectance factor A(%) = a(%) + b( %/count )C(counts)
2. The tabulated values of the slope and intercept are taken from the appendices to NOAA Technical Memorandum 107, "Data Extraction and Calibration of TIROS-N/NOAA Radiometers."(Lauritson et al. 1979)
3. The above regression parameters can be used to determine the filtered and spectral radiances of the earth-atmosphere scene using Eqns. 10 and 11 and the data shown in Table 10.

Table 15. AVHRRs onboard the various NOAA satellites

| Satellite | AVHRR model | Number of channels | Identification | Approximate date of calibration |
|---|---|---|---|---|
| NOAA-6 | 1 | 4 | FM 103 | March 1978 |
| NOAA-7 | 2 | 5 | FM 201 | June 1978 |
| NOAA-8 | 1 | 4 | FM 102 | June 1978 |
| NOAA-9 | 2 | 5 | FM 202 | February 1980 |
| NOAA-10 | 1 | 4 | FM 101 | July 1980 |

Note: The entries in the identification column are taken from the "Alignment and Calibration Data Book" for the various AVHRRs published by ITT Aerospace/Optical Division under contract with the Goddard Space Flight Center, National Aeronautics and Space Administration, Greenbelt, Maryland.

the Advanced Very High Resolution Radiometer gathered from diverse sources. We have attempted to elucidate the underlying physical principles and illustrate various laboratory procedures. It is hoped the information we have provided will be helpful to users of AVHRR data.

We feel it may be physically more meaningful to present the pre-launch calibration results in terms of the radiance of the integrating sphere rather than in terms of the reflectance factor; this approach would remove the dependence on the extraterrestrial solar spectral irradiance data. In the event the calibration in terms of the reflectance factor is continued, we suggest that it should be performed using the Neckel and Labs(1984) solar spectral irradiance data which are gaining acceptance amongst the scientific community; it is our understanding that these data have already been used in the calibration of the AVHRR scheduled to be part of the payload onboard NOAA-H.

In view of the increasing use of the AVHRR visible and near-infrared data in radiometric studies of the earth-atmosphere system, the feasibility of onboard calibration or stability monitoring of the next generation AVHRRs was explored through an "improvement study" at ITT/Aerospace-Optical Division, but was not pursued because of considerations based on the cost of such operations, and associated scheduling and technical difficulties(T.Wrublewski, personal communication).

Acknowledgments

The author wishes to place on record his sincere appreciation for Dr.Larry L. Stowe, NOAA/NESDIS, who suggested that this work be undertaken. He is thankful to Drs.Abel, Gallo, Gutman, Jacobowitz, McClain, Weinreb, and Wrublewski, NOAA/NESDIS, and to Dr.Koczar, ITT/Aerospace-Optical Division for their constructive criticism and comments. This work was completed while the author held a NOAA/NRC Resident Research Associateship at the National Environmental Satellite, Data, and Information Service, Washington, D.C.20233.

## References


Air Force 1965 Handbook of Geophysics and Space Physics. (Editor:Shea L. Valley), Air Force Cambridge Laboratories, Office of Aerospace Research, United States Air Force.

ITT 1980 Advanced Very High Resolution Radiometer (Model 2) for the TIROS "N" Spacecraft, Alignment and Calibration Data Book, AVHRR/2, Flight Model SN 202, ITT Aerospace/Optical Division, Fort Wayne, Indiana

Lauritson,L.,. Nelson,G.J., and Porto,F.W. 1979 Data Extraction and Calibration of TIROS-N/NOAA Radiometers. NOAA Technical Memorandum NESS 107, United States Department of Commerce, NOAA/NESS

Neckel,H., and Labs,D 1984 The solar radiation between 3300 and 12500A. Solar Physics. 90, 205-208

Price,J.B. 1987 Calibratin of satellite radiometers and comparison of vegetation indices. Remote Sens. Environ., 21, 15-27

Rossow,W.R., Kinsella,E., Wolf,A and Gardner,L 1985 Description of reduced radiance data, International Satellite Cloud Climatology Project(ISCCP), WMO/TD-No.58

Schwalb,A. 1978 The TIROS-N/NOAA Satellite Series, NOAA

Technical Memorandum NESS 95, United States Department of Commerce, NOAA/NESDIS

Thekaekara,M.P. 1974 Extraterrestrial solar spectrum. Appl. Opt., 13,518-522

# Appendix A: Tables of Normalized Response Functions

TABLE 1. NORMALIZED RESPONSE FUNCTIONS: NOAA -6

| WAVELENGTH(μM) | CHANNEL 1 | CHANNEL 2 |
|---|---|---|
| 0.5000 | 0.0000 | 0.0000 |
| 0.5100 | 0.0000 | 0.0000 |
| 0.5200 | 0.0000 | 0.0000 |
| 0.5300 | 0.0000 | 0.0000 |
| 0.5400 | 0.0000 | 0.0000 |
| 0.5500 | 0.0000 | 0.0000 |
| 0.5600 | 0.0710 | 0.0000 |
| 0.5700 | 0.4490 | 0.0000 |
| 0.5800 | 0.7390 | 0.0000 |
| 0.5900 | 0.8130 | 0.0000 |
| 0.6000 | 0.8060 | 0.0000 |
| 0.6100 | 0.8620 | 0.0000 |
| 0.6200 | 0.9190 | 0.0000 |
| 0.6300 | 0.9590 | 0.0000 |
| 0.6400 | 1.0000 | 0.0000 |
| 0.6500 | 0.9980 | 0.0000 |
| 0.6600 | 0.9970 | 0.0000 |
| 0.6700 | 0.8470 | 0.0000 |
| 0.6800 | 0.6980 | 0.0000 |
| 0.6900 | 0.3250 | 0.0000 |
| 0.7000 | 0.1320 | 0.0080 |
| 0.7100 | 0.0550 | 0.2600 |
| 0.7200 | 0.0270 | 0.6170 |
| 0.7300 | 0.0130 | 0.8200 |
| 0.7400 | 0.0070 | 0.9140 |
| 0.7500 | 0.0000 | 0.9430 |
| 0.7600 | 0.0000 | 0.9370 |
| 0.7700 | 0.0000 | 0.9970 |
| 0.7800 | 0.0000 | 1.0000 |
| 0.7900 | 0.0000 | 0.9250 |
| 0.8000 | 0.0000 | 0.8840 |
| 0.8100 | 0.0000 | 0.8490 |
| 0.8200 | 0.0000 | 0.8130 |
| 0.8300 | 0.0000 | 0.8010 |
| 0.8400 | 0.0000 | 0.7890 |
| 0.8500 | 0.0000 | 0.7840 |
| 0.8600 | 0.0000 | 0.7790 |
| 0.8700 | 0.0025 | 0.7630 |
| 0.8800 | 0.0050 | 0.7480 |
| 0.8900 | 0.0110 | 0.7420 |
| 0.9000 | 0.0170 | 0.7350 |
| 0.9100 | 0.0350 | 0.6850 |
| 0.9200 | 0.0480 | 0.6580 |
| 0.9300 | 0.0380 | 0.6320 |
| 0.9400 | 0.0180 | 0.6120 |
| 0.9500 | 0.0060 | 0.6010 |
| 0.9600 | 0.0020 | 0.5940 |
| 0.9700 | 0.0000 | 0.5820 |
| 0.9800 | 0.0000 | 0.5420 |
| 0.9900 | 0.0000 | 0.4710 |
| 1.0000 | 0.0000 | 0.3480 |
| 1.0100 | 0.0000 | 0.2180 |
| 1.0200 | 0.0000 | 0.1200 |
| 1.0300 | 0.0000 | 0.0620 |
| 1.0400 | 0.0000 | 0.0300 |
| 1.0500 | 0.0000 | 0.0130 |
| 1.0600 | 0.0000 | 0.0060 |
| 1.0700 | 0.0000 | 0.0030 |

TABLE 2. NORMALIZED RESPONSE FUNCTIONS: NOAA -7

| WAVELENGTH(μM) | CHANNEL 1 | CHANNEL 2 |
|---|---|---|
| 0.5000 | 0.0000 | 0.0000 |
| 0.5100 | 0.0032 | 0.0000 |
| 0.5200 | 0.0030 | 0.0000 |
| 0.5300 | 0.0028 | 0.0000 |
| 0.5400 | 0.0025 | 0.0000 |
| 0.5500 | 0.0047 | 0.0000 |
| 0.5600 | 0.1010 | 0.0000 |
| 0.5700 | 0.4740 | 0.0000 |
| 0.5800 | 0.7230 | 0.0000 |
| 0.5900 | 0.7870 | 0.0000 |
| 0.6000 | 0.7740 | 0.0380 |
| 0.6100 | 0.7930 | 0.0300 |
| 0.6200 | 0.8610 | 0.0250 |
| 0.6300 | 1.0000 | 0.0100 |
| 0.6400 | 0.9440 | 0.0000 |
| 0.6500 | 0.9420 | 0.0070 |
| 0.6600 | 0.9510 | 0.0060 |
| 0.6700 | 0.9770 | 0.0050 |
| 0.6800 | 0.7230 | 0.0050 |
| 0.6900 | 0.3450 | 0.0090 |
| 0.7000 | 0.1470 | 0.1010 |
| 0.7100 | 0.0710 | 0.4120 |
| 0.7200 | 0.0420 | 0.7330 |
| 0.7300 | 0.0270 | 0.9070 |
| 0.7400 | 0.0170 | 0.9660 |
| 0.7500 | 0.0120 | 0.9920 |
| 0.7600 | 0.0095 | 1.0000 |
| 0.7700 | 0.0100 | 0.9850 |
| 0.7800 | 0.0110 | 0.9930 |
| 0.7900 | 0.0070 | 0.9260 |
| 0.8000 | 0.0000 | 0.9410 |
| 0.8100 | 0.0000 | 0.9260 |
| 0.8200 | 0.0000 | 0.8700 |
| 0.8300 | 0.0000 | 0.8700 |
| 0.8400 | 0.0000 | 0.8710 |
| 0.8500 | 0.0000 | 0.8700 |
| 0.8600 | 0.0000 | 0.8760 |
| 0.8700 | 0.0000 | 0.8680 |
| 0.8800 | 0.0000 | 0.8720 |
| 0.8900 | 0.0000 | 0.8590 |
| 0.9000 | 0.0000 | 0.8450 |
| 0.9100 | 0.0000 | 0.8360 |
| 0.9200 | 0.0000 | 0.8230 |
| 0.9300 | 0.0000 | 0.7890 |
| 0.9400 | 0.0000 | 0.7820 |
| 0.9500 | 0.0000 | 0.7700 |
| 0.9600 | 0.0000 | 0.7630 |
| 0.9700 | 0.0000 | 0.7290 |
| 0.9800 | 0.0000 | 0.6080 |
| 0.9900 | 0.0000 | 0.4250 |
| 1.0000 | 0.0000 | 0.2500 |
| 1.0100 | 0.0000 | 0.1360 |
| 1.0200 | 0.0000 | 0.0730 |
| 1.0300 | 0.0000 | 0.0400 |
| 1.0400 | 0.0000 | 0.0230 |
| 1.0500 | 0.0000 | 0.0140 |
| 1.0600 | 0.0000 | 0.0080 |
| 1.0700 | 0.0000 | 0.0000 |

TABLE 3. NORMALIZED RESPONSE FUNCTIONS: NOAA -8

| WAVELENGTH(μM) | CHANNEL 1 | CHANNEL 2 |
|---|---|---|
| 0.5000 | 0.0074 | 0.0000 |
| 0.5100 | 0.0037 | 0.0000 |
| 0.5200 | 0.0000 | 0.0000 |
| 0.5300 | 0.0000 | 0.0000 |
| 0.5400 | 0.0000 | 0.0000 |
| 0.5500 | 0.0048 | 0.0000 |
| 0.5600 | 0.0749 | 0.0000 |
| 0.5700 | 0.4284 | 0.0000 |
| 0.5800 | 0.6896 | 0.0000 |
| 0.5900 | 0.7853 | 0.0000 |
| 0.6000 | 0.7773 | 0.0000 |
| 0.6100 | 0.7777 | 0.0000 |
| 0.6200 | 0.8356 | 0.0000 |
| 0.6300 | 0.9197 | 0.0000 |
| 0.6400 | 0.9739 | 0.0000 |
| 0.6500 | 0.9480 | 0.0000 |
| 0.6600 | 0.9588 | 0.0000 |
| 0.6700 | 1.0000 | 0.0000 |
| 0.6800 | 0.8770 | 0.0000 |
| 0.6900 | 0.4789 | 0.0380 |
| 0.7000 | 0.2067 | 0.0761 |
| 0.7100 | 0.0928 | 0.3954 |
| 0.7200 | 0.0496 | 0.7559 |
| 0.7300 | 0.0214 | 0.9186 |
| 0.7400 | 0.0190 | 0.9770 |
| 0.7500 | 0.0100 | 0.9946 |
| 0.7600 | 0.0080 | 1.0000 |
| 0.7700 | 0.0091 | 0.9861 |
| 0.7800 | 0.0103 | 0.9601 |
| 0.7900 | 0.0090 | 0.9268 |
| 0.8000 | 0.0076 | 0.8879 |
| 0.8100 | 0.0098 | 0.8627 |
| 0.8200 | 0.0121 | 0.8175 |
| 0.8300 | 0.0093 | 0.8033 |
| 0.8400 | 0.0068 | 0.7891 |
| 0.8500 | 0.0091 | 0.7810 |
| 0.8600 | 0.0114 | 0.7729 |
| 0.8700 | 0.0117 | 0.7659 |
| 0.8800 | 0.0120 | 0.7589 |
| 0.8900 | 0.0183 | 0.7467 |
| 0.9000 | 0.0265 | 0.7344 |
| 0.9100 | 0.0384 | 0.7096 |
| 0.9200 | 0.0522 | 0.6848 |
| 0.9300 | 0.0491 | 0.6578 |
| 0.9400 | 0.0396 | 0.6309 |
| 0.9500 | 0.0203 | 0.6133 |
| 0.9600 | 0.0125 | 0.5956 |
| 0.9700 | 0.0095 | 0.5674 |
| 0.9800 | 0.0048 | 0.5412 |
| 0.9900 | 0.0022 | 0.4400 |
| 1.0000 | 0.0021 | 0.3388 |
| 1.0100 | 0.0000 | 0.2081 |
| 1.0200 | 0.0000 | 0.1162 |
| 1.0300 | 0.0000 | 0.0606 |
| 1.0400 | 0.0000 | 0.0310 |
| 1.0500 | 0.0000 | 0.0153 |
| 1.0600 | 0.0000 | 0.0077 |
| 1.0700 | 0.0000 | 0.0052 |

TABLE 4. NORMALIZED RESPONSE FUNCTIONS: NOAA -9

| WAVELENGTH(μM) | CHANNEL 1 | CHANNEL 2 |
|---|---|---|
| 0.5000 | 0.0000 | 0.0000 |
| 0.5100 | 0.0000 | 0.0000 |
| 0.5200 | 0.0000 | 0.0000 |
| 0.5300 | 0.0000 | 0.0000 |
| 0.5400 | 0.0006 | 0.0000 |
| 0.5500 | 0.0142 | 0.0000 |
| 0.5600 | 0.2060 | 0.0000 |
| 0.5700 | 0.5061 | 0.0000 |
| 0.5800 | 0.6818 | 0.0000 |
| 0.5900 | 0.8055 | 0.0000 |
| 0.6000 | 0.8150 | 0.0000 |
| 0.6100 | 0.7800 | 0.0000 |
| 0.6200 | 0.8125 | 0.0000 |
| 0.6300 | 0.8963 | 0.0000 |
| 0.6400 | 0.9111 | 0.0000 |
| 0.6500 | 0.8265 | 0.0000 |
| 0.6600 | 0.8090 | 0.0000 |
| 0.6700 | 0.8837 | 0.0000 |
| 0.6800 | 1.0000 | 0.0000 |
| 0.6900 | 0.8713 | 0.0044 |
| 0.7000 | 0.4710 | 0.0694 |
| 0.7100 | 0.2139 | 0.3559 |
| 0.7200 | 0.0979 | 0.6876 |
| 0.7300 | 0.0507 | 0.8586 |
| 0.7400 | 0.0294 | 0.9369 |
| 0.7500 | 0.0182 | 0.9859 |
| 0.7600 | 0.0133 | 1.0000 |
| 0.7700 | 0.0098 | 0.9825 |
| 0.7800 | 0.0074 | 0.9323 |
| 0.7900 | 0.0063 | 0.9003 |
| 0.8000 | 0.0060 | 0.8875 |
| 0.8100 | 0.0000 | 0.8899 |
| 0.8200 | 0.0000 | 0.9026 |
| 0.8300 | 0.0000 | 0.9108 |
| 0.8400 | 0.0000 | 0.9132 |
| 0.8500 | 0.0000 | 0.8863 |
| 0.8600 | 0.0000 | 0.8638 |
| 0.8700 | 0.0000 | 0.8504 |
| 0.8800 | 0.0000 | 0.8616 |
| 0.8900 | 0.0000 | 0.8729 |
| 0.9000 | 0.0000 | 0.8811 |
| 0.9100 | 0.0000 | 0.8632 |
| 0.9200 | 0.0000 | 0.8112 |
| 0.9300 | 0.0000 | 0.7500 |
| 0.9400 | 0.0000 | 0.7193 |
| 0.9500 | 0.0000 | 0.7084 |
| 0.9600 | 0.0000 | 0.7425 |
| 0.9700 | 0.0000 | 0.7251 |
| 0.9800 | 0.0000 | 0.5523 |
| 0.9900 | 0.0000 | 0.3120 |
| 1.0000 | 0.0000 | 0.1529 |
| 1.0100 | 0.0000 | 0.0759 |
| 1.0200 | 0.0000 | 0.0414 |
| 1.0300 | 0.0000 | 0.0200 |
| 1.0400 | 0.0000 | 0.0150 |
| 1.0500 | 0.0000 | 0.0107 |
| 1.0600 | 0.0000 | 0.0074 |
| 1.0700 | 0.0000 | 0.0057 |

TABLE 5. NORMALIZED RESPONSE FUNCTIONS: NOAA -10

| WAVELENGTH(μM) | CHANNEL 1 | CHANNEL 2 |
|---|---|---|
| 0.5000 | 0.0000 | 0.0000 |
| 0.5100 | 0.0000 | 0.0000 |
| 0.5200 | 0.0000 | 0.0000 |
| 0.5300 | 0.0000 | 0.0000 |
| 0.5400 | 0.0020 | 0.0000 |
| 0.5500 | 0.0030 | 0.0000 |
| 0.5600 | 0.0866 | 0.0000 |
| 0.5700 | 0.4870 | 0.0000 |
| 0.5800 | 0.7450 | 0.0000 |
| 0.5900 | 0.8210 | 0.0000 |
| 0.6000 | 0.8098 | 0.0000 |
| 0.6100 | 0.8580 | 0.0024 |
| 0.6200 | 0.9490 | 0.0048 |
| 0.6300 | 0.9956 | 0.0050 |
| 0.6400 | 0.9630 | 0.0053 |
| 0.6500 | 0.9490 | 0.0055 |
| 0.6600 | 1.0000 | 0.0057 |
| 0.6700 | 0.9920 | 0.0044 |
| 0.6800 | 0.6290 | 0.0031 |
| 0.6900 | 0.2730 | 0.0032 |
| 0.7000 | 0.1070 | 0.0034 |
| 0.7100 | 0.0530 | 0.0855 |
| 0.7200 | 0.0280 | 0.3680 |
| 0.7300 | 0.0180 | 0.6990 |
| 0.7400 | 0.0120 | 0.8750 |
| 0.7500 | 0.0080 | 0.9420 |
| 0.7600 | 0.0042 | 0.9780 |
| 0.7700 | 0.0010 | 1.0000 |
| 0.7800 | 0.0000 | 0.9733 |
| 0.7900 | 0.0000 | 0.9455 |
| 0.8000 | 0.0000 | 0.8980 |
| 0.8100 | 0.0000 | 0.8800 |
| 0.8200 | 0.0000 | 0.8750 |
| 0.8300 | 0.0000 | 0.8380 |
| 0.8400 | 0.0000 | 0.8520 |
| 0.8500 | 0.0000 | 0.8470 |
| 0.8600 | 0.0000 | 0.8230 |
| 0.8700 | 0.0000 | 0.7900 |
| 0.8800 | 0.0000 | 0.8230 |
| 0.8900 | 0.0000 | 0.8070 |
| 0.9000 | 0.0000 | 0.7750 |
| 0.9100 | 0.0000 | 0.7600 |
| 0.9200 | 0.0000 | 0.6900 |
| 0.9300 | 0.0000 | 0.6720 |
| 0.9400 | 0.0000 | 0.6680 |
| 0.9500 | 0.0000 | 0.6580 |
| 0.9600 | 0.0000 | 0.6080 |
| 0.9700 | 0.0000 | 0.5730 |
| 0.9800 | 0.0000 | 0.5220 |
| 0.9900 | 0.0000 | 0.3830 |
| 1.0000 | 0.0000 | 0.2250 |
| 1.0100 | 0.0000 | 0.1310 |
| 1.0200 | 0.0000 | 0.0690 |
| 1.0300 | 0.0000 | 0.0380 |
| 1.0400 | 0.0000 | 0.0210 |
| 1.0500 | 0.0000 | 0.0126 |
| 1.0600 | 0.0000 | 0.0079 |
| 1.0700 | 0.0000 | 0.0054 |

## NOAA SCIENTIFIC AND TECHNICAL PUBLICATIONS

*The National Oceanic and Atmospheric Administration* was established as part of the Department of Commerce on October 3, 1970. The mission responsibilities of NOAA are to assess the socioeconomic impact of natural and technological changes in the environment and to monitor and predict the state of the solid Earth, the oceans and their living resources, the atmosphere, and the space environment of the Earth.

The major components of NOAA regularly produce various types of scientific and technical information in the following kinds of publications:

PROFESSIONAL PAPERS—Important definitive research results, major techniques, and special investigations.

CONTRACT AND GRANT REPORTS—Reports prepared by contractors or grantees under NOAA sponsorship.

ATLAS—Presentation of analyzed data generally in the form of maps showing distribution of rainfall, chemical and physical conditions of oceans and atmosphere, distribution of fishes and marine mammals, ionospheric conditions, etc.

TECHNICAL SERVICE PUBLICATIONS—Reports containing data, observations, instructions, etc. A partial listing includes data serials; prediction and outlook periodicals; technical manuals, training papers, planning reports, and information serials; and miscellaneous technical publications.

TECHNICAL REPORTS—Journal quality with extensive details, mathematical developments, or data listings.

TECHNICAL MEMORANDUMS—Reports of preliminary, partial, or negative research or technology results, interim instructions, and the like.

**NATIONAL ENVIRONMENTAL SATELLITE, DATA, AND INFORMATION SERVICE**
**NATIONAL OCEANIC AND ATMOSPHERIC ADMINISTRATION**
**U.S. DEPARTMENT OF COMMERCE**
**Washington, D.C. 20233**